Research Square

Preprints are preliminary reports that have not undergone peer review.
They should not be considered conclusive, used to inform clinical practice,
or referenced by the media as validated information.

What district damage statistics can identify: joint Bayesian inference of intensity and masonry vulnerability after the 2005 Kashmir earthquake

Syed Sajid Hussain

syedsajid0529@gmail.com

Sharif University of Technology

Research Article

Keywords: Empirical fragility, Macroseismic vulnerability, Bayesian identifiability, ShakeMap, Stone masonry, 2005 Kashmir earthquake

Posted Date: November 17th, 2026

DOI: https://doi.org/10.21203/rs.3.rs-11509792/v1

License: This work is licensed under a Creative Commons Attribution 4.0 International License.
Read Full License

Additional Declarations: No competing interests reported.

What district damage statistics can identify: joint Bayesian inference of intensity and masonry vulnerability after the 2005 Kashmir earthquake

Syed Sajid Hussain

Department of Civil Engineering, Sharif University of Technology, Tehran, Iran
E-mail: syedsajid0529@gmail.com

Abstract The Kashmir Himalaya lies in a seismic gap capable of a great earthquake. Yet its risk models borrow fragility functions derived for Nepalese and European buildings. Local functions are lacking since the 2005 M_w 7.6 Kashmir earthquake left only district counts of destroyed and damaged dwellings. This study uses these counts to derive fragility functions for Himalayan masonry and to identify what such data support. Counts for 787,583 dwellings in eight Pakistan-administered districts were combined with census wall materials and ShakeMap intensity. A hierarchical Bayesian form of the macroseismic method treated the intensity field as uncertain. The model was tested by leave-one-district-out prediction, on official damage counts from Indian Jammu and Kashmir and on synthetic data. For rubble stone, the dominant wall type, the vulnerability index was 0.96 (90% interval 0.81–1.10), at or slightly above the European reference of 0.873. The estimate held under neutral priors, a damage-free intensity field and a terrain term. A difference between rubble stone and brick masonry was not established, since terrain-linked intensity errors could produce it. Modeling the reporting categories, rather than calibration, gave most of the predictive skill. In Indian Kashmir, fully damaged houses fell within the predicted ranges, whereas partial damage in Kupwara was under-predicted. Census data show brick and block masonry replacing timber-walled houses, raising expected heavy damage unless timber walls are highly vulnerable. The results show what aggregated damage reports can identify, and that finer damage records or more precise district intensities alone would narrow the class indices only modestly.

Keywords Empirical fragility · Macroseismic vulnerability · Bayesian identifiability · ShakeMap · Stone masonry · 2005 Kashmir earthquake

1 Introduction

The 8 October 2005 M_w 7.6 Kashmir earthquake killed more than 73,000 people in Pakistan alone and left about 2.8 million without shelter (ADB and World Bank 2005). In Indian Jammu and Kashmir, more than 100,000 houses were damaged in the Baramulla and Kupwara districts alone (UNI 2006). It ruptured the Balakot–Bagh fault (Kaneda et al. 2008) at the western end of the Kashmir seismic gap. This segment of the Himalayan front lies between the rupture zones of the 1555 Kashmir and 1905 Kangra earthquakes and is considered capable of a great earthquake (Thakur et al. 2006; Hough et al. 2009; Qader et al. 2026). Along much of the Himalayan arc, the slip accumulated since the last great earthquakes is sufficient for one or more such events (Bilham et al. 2001). Rapid urbanization increases the number of people and buildings exposed to them (Bilham 2009). Almost all of the destruction in 2005 was suffered by low-rise, non-engineered dwellings of rubble-stone, mud, concrete-block and brick masonry (EERI 2005; Rai and Murty 2006; Maqsood and Schwarz 2008). The vulnerability of this housing stock therefore controls much of the earthquake risk of the region.

Regional seismic risk assessment combines a hazard model, an exposure model and fragility or vulnerability functions, which give the probability of each damage state at a given ground-motion intensity. Risk engines such as OpenQuake (Silva et al. 2014) and global vulnerability models (Martins and Silva 2021) require such functions for every building class. Fragility functions can be derived empirically from damage observed after past earthquakes (Rossetto and Elnashai 2003; Rossetto et al. 2014), analytically from structural models, or from expert judgment. The macroseismic method of Lagomarsino and Giovinazzi (2006) derives vulnerability curves from the damage probability matrices implicit in the European Macroseismic Scale (Grünthal 1998), and its heuristic extension provides fragility curves for masonry typologies (Lagomarsino et al. 2021). Empirical functions are preferred where adequate data exist, since they reflect the materials, workmanship and failure modes of the actual stock. Their reliability depends on the resolution of the damage data and on the accuracy of the intensity assigned to each observation.

Despite the scale of the disaster and the continuing hazard, fragility functions specific to the housing of the Kashmir Himalaya are lacking. Regional risk studies borrow functions derived for other stocks, mainly Nepalese stone masonry after the 2015 Gorkha earthquake (Gautam 2018; Giordano et al. 2021). Others use the vulnerability classes of the European Macroseismic Scale, defined for European building types, as in the field survey of Maqsood and Schwarz (2008), which placed the regional building types in lower vulnerability classes than is typical for each type. Still others rely on index-based vulnerability ranking without probabilistic damage functions (Fayaz et al. 2023). The only empirical fragility functions identified in the literature for the region are those for brick masonry after the moderate 2019 Mirpur earthquake (Rafi et al. 2023). Borrowed functions therefore assume a resemblance between the source and local stocks in materials, workmanship and roof weight that has not been tested against local damage data.

Experimental studies have characterized the regional masonry directly. Shake-table tests on reduced-scale rubble-stone models from the region showed damage and collapse at low input accelerations, and a large improvement from thin reinforced-concrete bands and vertical elements (Ali et al. 2013). A one-third-scale half-dressed stone model collapsed at a table acceleration of 0.20 g, and analytical fragility functions were derived from it (Ahmad et al. 2012c). These studies describe the capacity of individual specimens under controlled excitation. The population of dwellings damaged in an actual earthquake varies in materials, workmanship, roof weight and maintenance, and its fragility can only be obtained by calibration against observed damage.

Two obstacles explain the gap. The first is data. Where building-by-building surveys exist, as after the 2009 L'Aquila earthquake (Del Gaudio et al. 2017) and in other Italian damage databases (Rota et al. 2008; Rosti et al. 2021), empirical fragility curves can be fitted for each typology (Rossetto et al. 2014; Lallemant et al. 2015); however, the public record of the 2005 earthquake contains no such survey. Reconnaissance studies documented the damage mechanisms of the regional stock in detail (Bothara and Hiçyılmaz 2008; Rossetto and Peiris 2009; Naseer et al. 2010), although not in a form from which fragility functions can be fitted. Its most complete quantitative record is a table of destroyed and damaged dwellings by district, compiled for the reconstruction needs assessment (ADB and World Bank 2005). The later reconstruction survey classified about 463,000 houses as destroyed and eligible for reconstruction grants (Arshad and Athar 2013), which shows that the reported categories depended on the purpose of each survey. The second obstacle is the shaking itself. Only three accelerograph records exist, all inside buildings at 35–120 km from the epicenter (Durrani et al. 2005; Maqsood and Schwarz 2008). The USGS ShakeMap Atlas reconstruction of the event contains no instrumental records and rests on 351

macroseismic observations (USGS 2020). On the Indian side, field intensities were assigned on the Medvedev–Sponheuer–Karnik (MSK) scale for a few towns only (Rai and Murty 2006). Where observations are sparse, ShakeMap intensities revert to ground-motion model predictions with large uncertainty (Worden et al. 2020). Recent far-field records elsewhere show that such predictions can be biased in complex terrain and sedimentary basins (Ornthammarath et al. 2025). Felt reports, which could supplement them, are themselves unevenly distributed, with response rates that vary strongly between regions (Knodel et al. 2026).

Bayesian methods have been developed to account for such uncertainties. Straub and Der Kiureghian (2008) showed that common ground-motion and model uncertainties make the damage observations of one earthquake statistically dependent, a dependence that must be modeled to avoid overconfident fragility estimates. Koutsourelakis (2010) proposed a Bayesian framework for multi-dimensional fragility surfaces. Ioannou et al. (2015) showed with simulated damage databases that ground-motion variability flattens empirical fragility curves, that epistemic uncertainty in ground-motion prediction can change them considerably, and that aggregating damage observations substantially increases their uncertainty. Ioannou et al. (2020) then applied a Bayesian framework to the municipality-level damage database of the 1980 Irpinia earthquake, treating the intensity of each municipality as uncertain. The fragility curves changed little with model complexity, whereas the variability of the data between municipalities had to be modeled explicitly. Both studies work with damage observations recorded by building class and damage state.

For collapse alone, Jaiswal et al. (2011) combined expert-elicited fragility in macroseismic intensity with field collapse rates in a Bayesian update, an approach similar to the present one, although applied to individual building types rather than to mixed administrative units. Aggregated statistics also underlie global empirical loss models, such as the country-level fatality model of Jaiswal and Wald (2010). Where damage observations are incomplete, geospatial models can combine field surveys with damage forecasts and remote sensing to estimate damage over a region (Loos et al. 2020). The record of the 2005 Kashmir earthquake is poorer than the data of these studies in three respects. Each district mixes building classes; the reported categories ("destroyed", "damaged") do not correspond to the damage grades of a standard scale; and the intensity field is itself partly derived from damage. Inferring the vulnerability of each class from district totals is then an ecological inference problem, in which associations between aggregates need not hold for their components (Goodman 1953; King 1997). Under these conditions, the quantities that such data can identify remain unclear.

A further gap concerns construction practice. The traditional timber-reinforced systems taq and dhajji-dewari were reported to perform better than unreinforced masonry in 2005 (Rai and Murty 2006; Ahmad et al. 2017), and dhajji-dewari has been tested in the laboratory (Ali et al. 2012; Ali et al. 2017), with simplified tools proposed for its seismic analysis and design (Ahmad et al. 2012a). Census data show a decline of timber-walled housing in the Kashmir Valley over the following years (ORGI 2001a; ORGI 2011), and the effect of this change on expected damage has not been quantified.

In this study, these questions are addressed with a hierarchical Bayesian model built on the macroseismic method of Lagomarsino and Giovinazzi (2006), in which intensity and vulnerability are inferred jointly. A quantity is regarded as identified when the data, rather than its prior, determine its value, and the quantities identified by the data are separated from those fixed by the priors. They are examined in order of decreasing information: the vulnerability of the dominant class given an intensity field, the contrast between the two classes whose shares vary most between districts, and the vulnerabilities of minority classes. A likelihood is formulated for district damage

counts with uncertain intensity, unknown reporting categories and district overdispersion. An identifiability analysis is carried out with neutral priors, a damage-free intensity field and synthetic tests, including intensity errors aligned with wall composition. Damage-calibrated vulnerability indices and fragility functions are derived for Himalayan rubble-stone masonry, in intensity and in peak ground acceleration. The model is scored against six alternative predictors and tested out of sample on official damage counts from Indian Jammu and Kashmir. Finally, the value of sub-district damage records is estimated, dhajji-dewari is placed on the same vulnerability scale, and the effect of recent housing change on expected damage is assessed.

2 Materials and methods

2.1 Housing stock of the western Himalaya

Rural housing in the affected districts consists predominantly of one- and two-story dwellings with load-bearing walls of rubble stone, concrete block, burnt brick, or mud and unburnt brick. Roofs are of timber and mud, metal sheet or reinforced concrete (ADB and World Bank 2005; Maqsood and Schwarz 2008). The needs assessment describes the typical *katcha* dwelling as having "mud or stone rubble walls with a flat mud roof supported on pole beams". It notes that "virtually none of the housing in affected areas has seismic consideration in design" (ADB and World Bank 2005). Stone masonry in the region is laid in lean cement–sand or mud mortar, and sometimes without mortar. On the basis of their field survey, Maqsood and Schwarz (2008) assigned the regional building types to lower EMS-98 vulnerability classes than is typical for each type. Shake-table tests on reduced-scale rubble-stone models from the region showed damage and collapse at low input accelerations, and a large improvement from thin reinforced-concrete bands and vertical elements (Ali et al. 2013). A one-third-scale half-dressed stone model collapsed in the third test run, at a table acceleration of 0.20 g, and analytical fragility functions were derived from it (Ahmad et al. 2012c).

Two traditional timber-reinforced systems are widespread in the Kashmir Valley (Langenbach 1990; Dhandapany and Menon 2019). *Taq* has thick brick or stone walls laced with horizontal timber bands. *Dhajji-dewari* is a braced timber frame with small masonry infill panels. Both were reported to perform better than unreinforced masonry in 2005 (Rai and Murty 2006; Ahmad et al. 2017). Dhajji-dewari has been characterized by full-scale quasi-static tests (Ali et al. 2012) and by shake-table tests on single-story (Ali et al. 2017) and two-story structures (Ali et al. 2021). It has also been studied with numerical models (Ahmad et al. 2012a; Harathi and Choudhury 2026). Ahmad et al. (2012b) derived analytical fragility functions in terms of peak ground acceleration (PGA) and estimated that collapse of single-story structures requires about 0.9 g. Dhandapany and Menon (2019) interpret the timber bands of taq as a form of multi-level isolation and call for experimental study. No quantitative capacity data for taq are available.

2.2 Macroseismic vulnerability model

In the macroseismic method (Lagomarsino and Giovinazzi 2006), the mean EMS-98 (Grünthal 1998) damage grade μ_D of a building class is a function of the macroseismic intensity I and a vulnerability index V:

$$\mu_D = 2.5\left[1 + \tanh\left(\frac{I + 6.25\,V - 13.1}{Q}\right)\right] \tag{1}$$

where Q is a ductility index, equal to 2.3 for buildings not specifically designed for ductile behavior. A higher V means a more vulnerable class: an increase of 0.16 in V has the same effect on μ_D as an increase of one intensity degree. The probability of damage grade D_k ($k = 0, \ldots, 5$) follows the binomial distribution

$$p_k = \frac{5!}{k!\ (5-k)!}(\mu_D/5)^k(1-\mu_D/5)^{5-k} \qquad (2)$$

Lagomarsino and Giovinazzi (2006) also refer to a beta distribution that allows a different scatter; it is tested here as a sensitivity case. Representative indices and probable ranges V^-–V^+ are given for each building typology (Lagomarsino and Giovinazzi 2006, Table 3). For example, rubble stone (typology M1) has $V = 0.873$ (0.81–0.98), simple stone (M3) 0.74, adobe (M2) 0.84 (0.687–0.98), and reinforced or confined masonry (M7) 0.451 (0.33–0.633). The heuristic vulnerability model of Lagomarsino et al. (2021) extends this framework to fragility curves for masonry typologies, and Lagomarsino and Giovinazzi (2006) also correlate V and Q with the parameters of a bilinear capacity curve (Sect. 2.4.7), a correlation used here to place dhajji-dewari on the same vulnerability scale. Since Eq. (1) depends on I and V only through $I + 6.25\,V$, damage observations alone cannot separate a stronger shaking from a weaker stock. A district with heavy damage may have been shaken strongly or built poorly, and only independent information on the intensity, differences in the composition of the stock between districts or the priors can distinguish the two.

2.3 Data

2.3.1 District damage statistics

The Preliminary Damage and Needs Assessment of the Asian Development Bank and the World Bank (ADB and World Bank 2005) reports, for the eight most affected districts, the housing stock and the numbers of dwellings destroyed and damaged as of 9 November 2005 (Table 1). In Table 1, AJK denotes Azad Jammu and Kashmir and KP Khyber Pakhtunkhwa; Poonch (AJK) is distinct from Punch district in Indian Jammu and Kashmir. Dwellings "damaged in excess of 40%" were classified as destroyed. The 787,583 dwellings include 203,579 destroyed and 196,573 damaged units, and the share destroyed ranges from 5% in Abbottabad to 64% in Batagram. The figures are preliminary and were compiled by government agencies during the relief phase. Maqsood and Schwarz (2008) attribute the damage in the areas they surveyed primarily to ground shaking. EERI (2006), however, reports that many buildings on or near slopes were destroyed by landsliding or subsidence; the counts therefore include some ground-failure losses. Over-reporting in the "destroyed" category cannot be excluded where compensation depended on it (Sect. 3.14). These limitations are represented in the model through the reporting parameters and an overdispersion term (Sect. 2.4).

Table 1 Housing stock, reported damage and ShakeMap intensity at the district headquarters (HQ) (ADB and World Bank 2005; USGS 2020)

District	Province	Dwellings	Destroyed	Damaged	Destroyed (%)	ShakeMap MMI at HQ	SD
Muzaffarabad	AJK	123,679	69,943	28,278	56.6	8.7	0.76
Bagh	AJK	59,623	33,806	21,208	56.7	7.4	0.77
Poonch	AJK	61,678	12,823	38,882	20.8	6.9	0.73
Shangla	KP	67,003	15,661	10,821	23.4	5.6	0.96
Mansehra	KP	203,109	31,323	43,282	15.4	7.3	0.69
Kohistan	KP	74,087	4,350	18,395	5.9	5.4	0.96
Abbottabad	KP	153,819	6,961	27,051	4.5	6.7	0.78
Batagram	KP	44,585	28,712	8,656	64.4	7.6	0.80
Total		787,583	203,579	196,573	25.8		

2.3.2 Intensity

The intensity field is the USGS ShakeMap Atlas reconstruction of the event (event usp000e12e; ShakeMap 4.0.2, processed 2020) (USGS 2020; Worden et al. 2020). It is constrained by 351 macroseismic observations (330 field intensities and 21 "Did You Feel It?" reports) and no instrumental records. Gridded Modified Mercalli intensity (MMI) and its standard deviation (0.033° spacing) were extracted for the whole region (Fig. 1). Fig. 1 also shows the calibration districts with their destroyed shares, the districts of Indian Jammu and Kashmir, the two Indian districts used for the out-of-sample test (Sect. 3.8) and the rupture plane fitted to the ShakeMap distances (Sect. 2.3.4). Neelum is included with Muzaffarabad, with which it was reported. The field intensities were assigned largely from observed building damage. Six of the eight district headquarters have such an observation within 2.4 km, and the two published field estimates for Muzaffarabad, MMI VIII–IX (EERI 2005) and EMS-98 IX (Maqsood and Schwarz 2008), are themselves entries of the station list. The ShakeMap prior is therefore not independent of the damage data. Kim and Elnashai (2009) reconstructed the distribution of shaking from the strong-motion and damage evidence available for the event; however, no independent instrumental field exists. The reference model does not use the Muzaffarabad estimates as additional constraints; their effect is tested as a sensitivity case, together with a doubled ShakeMap uncertainty (Sect. 3.3).

The only intensity information independent of building damage comes from the accelerographs. At Abbottabad (35 km, on alluvium, inside a building) peak horizontal accelerations of 0.231 g and 0.197 g were recorded (Durrani et al. 2005, as reported by Maqsood and Schwarz 2008). Their geometric mean, 0.213 g, corresponds to MMI 6.8 under the relation of Wald et al. (1999), which agrees closely with the later relation of Worden et al. (2012) for MMI ≥ V. This value enters the model as an anchor with a standard deviation of 0.8 intensity units, a conservative allowance for the scatter of the conversion and for the location of the instrument. On the Indian side, Rai and Murty (2006) assigned MSK VIII to Uri, VII to Baramulla and Kupwara, and V to Srinagar. Musson et al. (2010, Table 2) propose a one-to-one correspondence of MMI and MSK with EMS-98 up to degree XI, and the three scales are treated here as equivalent.

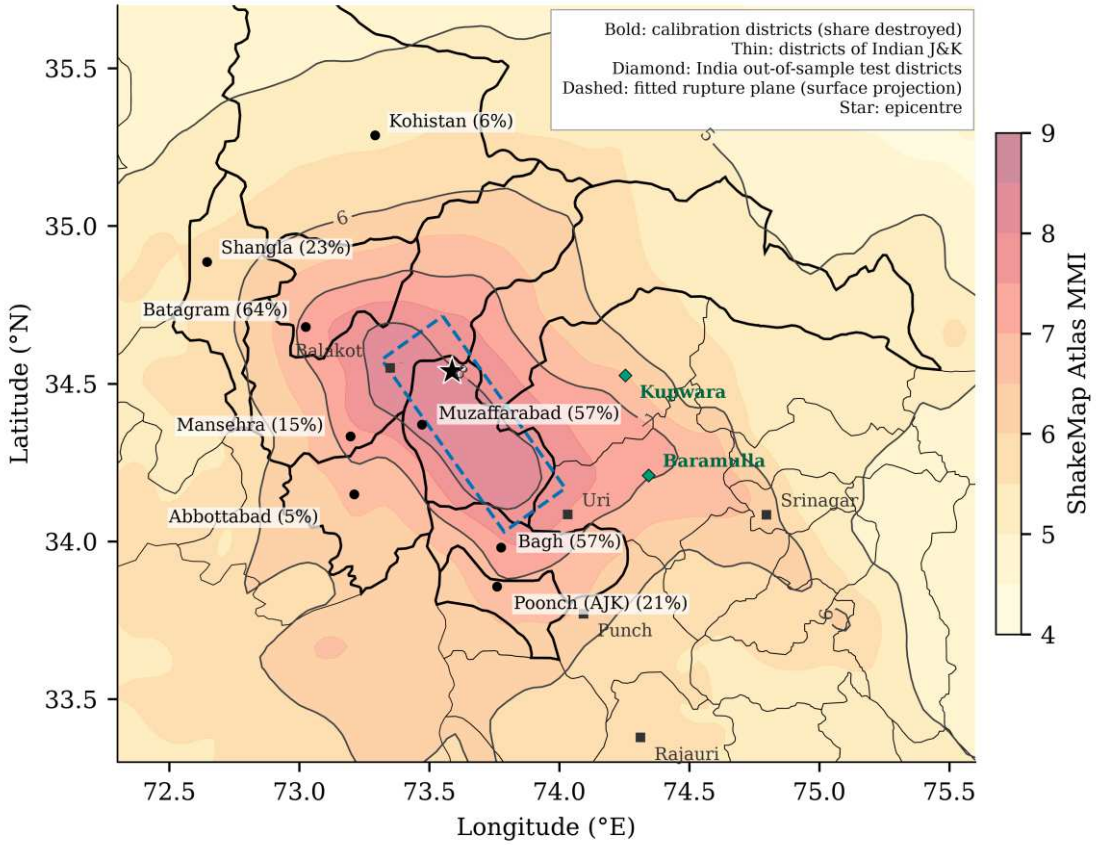


Fig. 1 Study area and ShakeMap Atlas intensity of the 2005 Kashmir earthquake (ADB and World Bank 2005; USGS 2020). Boundaries (Database of Global Administrative Areas, GADM 4.1) are shown only to locate the data and imply no position on any territorial claim

2.3.3 Exposure composition

For the five Khyber Pakhtunkhwa districts, the share of households by wall material comes from the district-level Pakistan Social and Living Standards Measurement (PSLM) Survey 2004–05 (FBS n.d.), conducted about a year before the earthquake (Table 2). The survey distinguishes burnt brick or block; mud or unburnt brick; wood or bamboo; and other. In these mountain districts the residual category is dominated by stone walls and is treated as rubble-stone masonry; a case with 20% of it reassigned to brick and block is tested in Sect. 3.3. The survey does not cover Azad Jammu and Kashmir. The three AJK districts are therefore assigned the average composition of the rural hill districts (Shangla, Batagram, and the rural parts of Mansehra and Abbottabad), and alternatives are tested in Sect. 3.3. Since the three AJK districts share one composition, any difference in their damage can only be explained by intensity, a constraint discussed in Sect. 3.15. For Indian Jammu and Kashmir, households by predominant wall material come from the Census of India 2001 (ORGI 2001a), and the distribution of census houses by tehsil (sub-district) (ORGI 2001b) separates the tehsils Uri and Karnah on the Line of Control, the de facto boundary between the Pakistani- and Indian-administered parts of Kashmir, from the rest of their districts. Each Line-of-Control tehsil takes the wall mix of its census houses, scaled to its share of the district households, and the rest of the district takes the remainder; the units of each district therefore add up to its household composition (Table 15).

Table 2 Wall-material composition of the calibration districts (% of households) and representative vulnerability indices (FBS n.d.; Lagomarsino and Giovinazzi 2006)

	Brick/block unreinforced masonry (URM)	**Mud/adobe**	**Timber-framed**	**Rubble stone**
Typology (Lagomarsino and Giovinazzi 2006)	M5–M6	M2	M7 (analogue)	M1
Representative V^*	0.678	0.84	0.451	0.873
Shangla	24.3	11.6	1.0	63.1
Mansehra	47.1	25.0	0.3	27.6
Abbottabad	51.7	8.1	0.0	40.2
Batagram	19.9	7.4	0.0	72.8
Kohistan	5.2	1.5	13.0	80.4
AJK districts (assumed)	26.2	13.8	0.3	59.8

2.3.4 Population-weighted intensity and rupture distance

Since damage is a convex function of intensity, the damage of a district differs from the damage at the intensity of its headquarters. Each district is therefore described by the distribution of ShakeMap MMI over its population, obtained by overlaying the 1-km WorldPop 2005 population grid (Tatem 2017) on the ShakeMap grid within the GADM 4.1 district boundaries (Table 3, Fig. 2). The population totals correspond to 5.9–9.0 persons per dwelling of Table 1. The difference from the headquarters value is large where the headquarters lie in the most strongly shaken valley: the population-weighted mean is 0.9 intensity units lower in Muzaffarabad (including Neelum) and 0.7 units lower in Batagram.

As a prior that uses no damage observations, the intensity prediction equation of Allen et al. (2012) for active crustal regions (AWW12) was evaluated for every population cell (Sect. 2.4.4); its population-weighted means are listed in Table 3. Intensity attenuation for Himalayan earthquakes is comparable to that in California (Szeliga et al. 2010), which supports the use of an active-crust relation here. To test whether ShakeMap bias depends on distance, a rectangular rupture plane was fitted to the regression distances listed for the 98 ShakeMap observations within 250 km (root-mean-square misfit 2.2 km), and the population-weighted rupture distance of every unit was computed (Table 3).

Table 3 Population-weighted intensity and rupture distance of the calibration districts (Tatem 2017; USGS 2020; Allen et al. 2012)

District	**Population (WorldPop 2005)**	**MMI at HQ**	**Population-weighted MMI, mean (10–90%)**	**SD**	**Damage-free field (AWW12)**	**Rupture distance (km)**
Muzaffarabad	724,000	8.7	7.8 (5.8–8.5)	0.85	7.8	15
Bagh	471,000	7.4	7.1 (6.6–7.6)	0.85	7.6	16
Poonch	419,000	6.9	6.7 (6.3–7.1)	0.88	7.2	27
Shangla	605,000	5.6	5.8 (5.5–6.3)	0.96	6.3	62
Mansehra	1,329,000	7.3	7.2 (6.1–8.2)	0.88	7.3	26
Kohistan	522,000	5.4	5.5 (5.0–6.1)	0.96	6.2	70
Abbottabad	1,085,000	6.7	6.7 (6.1–7.3)	0.85	6.9	35
Batagram	383,000	7.6	6.9 (6.3–7.6)	0.89	7.0	32

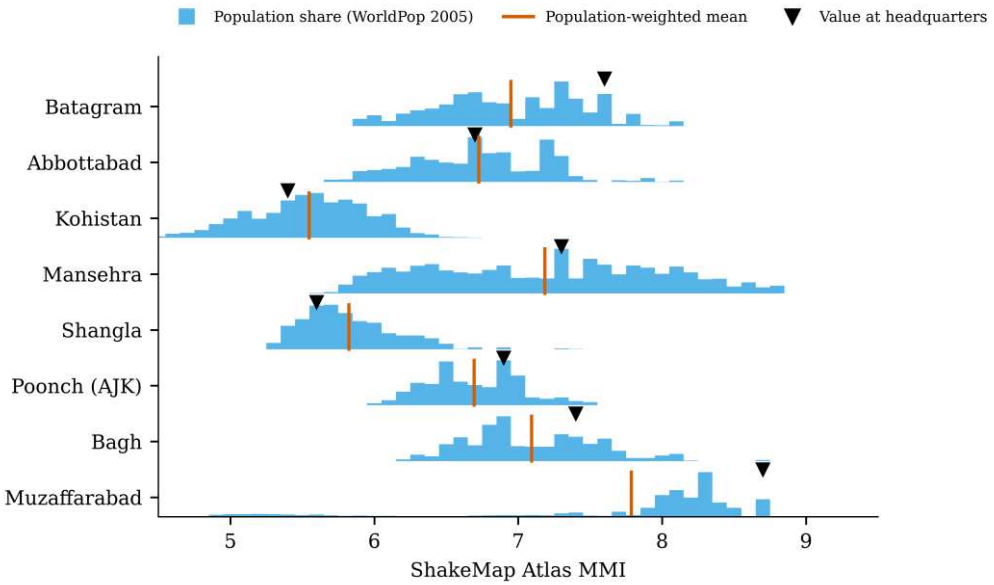


Fig. 2 Distribution of ShakeMap Atlas intensity over the 2005 population of the calibration districts (Tatem 2017; USGS 2020)

2.3.5 Reported losses in Indian Jammu and Kashmir

On the Indian side, the provisional figures of the relief phase conflict. On 12 October 2005 the Chief Minister reported 40,720 dwellings razed and 73,450 partially damaged in the state (AFP 2005). The Government of India situation report of 21 October gives 36,693 damaged structures in Kashmir division and 914 in Jammu division (Government of India 2005). Final figures by district were given by the Minister for Revenue and Rehabilitation in the J&K Legislative Assembly on 15 March 2006, as reported by the United News of India (UNI 2006). The state as a whole had 26,177 houses fully and 123,180 partially damaged. In Baramulla, about 15,000 houses were fully and 39,373 partially damaged. In Kupwara the figures were 9,305 and 55,076. Punch (J&K) had 8,072 houses fully or partially damaged. These final district figures are used here. Baramulla and Kupwara contain the Line-of-Control tehsils Uri and Karnah and account for 93% of the fully damaged houses of the state. The provisional Jammu-division figure of 914 is far below the final Punch figure alone and is not used. The ratio of partially to fully damaged houses is 2.6 in Baramulla and 5.9 in Kupwara, against about 1.0 for damaged to destroyed dwellings in the Pakistani assessment. This suggests that "partially damaged" was defined more inclusively by the Indian relief survey, which is allowed for in Sect. 2.4.7. Exposure comes from the Census of India 2001 (ORGI 2001c). The wall-material table counts 739,597 households in the Kashmir division units, 2% fewer than the 753,807 households of the Primary Census Abstract; the former is used throughout. Households rather than dwellings are the exposure unit on the Indian side.

2.3.6 Change of the Indian housing stock, 2001–2011

The Census of India 2011 reports households by predominant wall material in the same categories as 2001, with the addition of separate "stone packed" and "stone not packed with mortar" classes (ORGI 2011). The 2011 districts were merged into the 2001 districts (Baramulla with Bandipore, Srinagar with Ganderbal, Pulwama with Shupiyan, Anantnag with Kulgam) and the categories mapped to the four wall classes as in 2001. The census records only the materials of the walls and the roof. Qualitative field observations of recent construction in the Kashmir Valley, made during this study, indicate that timber-braced dwellings are being replaced by brick or block masonry with

reinforced-concrete floor slabs, some timber elements and large openings; these observations are not a survey and are used only to frame Sect. 3.11.2. The census therefore captures the change of wall material alone.

2.4 Model and analyses

Fig. 3 summarizes the data, the model and the analyses of this section. The district damage counts, the census compositions and the population-weighted ShakeMap intensities enter a hierarchical model in which the intensity of each district and the meaning of the reported categories are uncertain. The identifiability of its parameters is then examined, its predictions are scored against alternative predictors, and the calibrated functions are converted to peak ground acceleration, tested on the Indian districts and applied to the change of the housing stock.

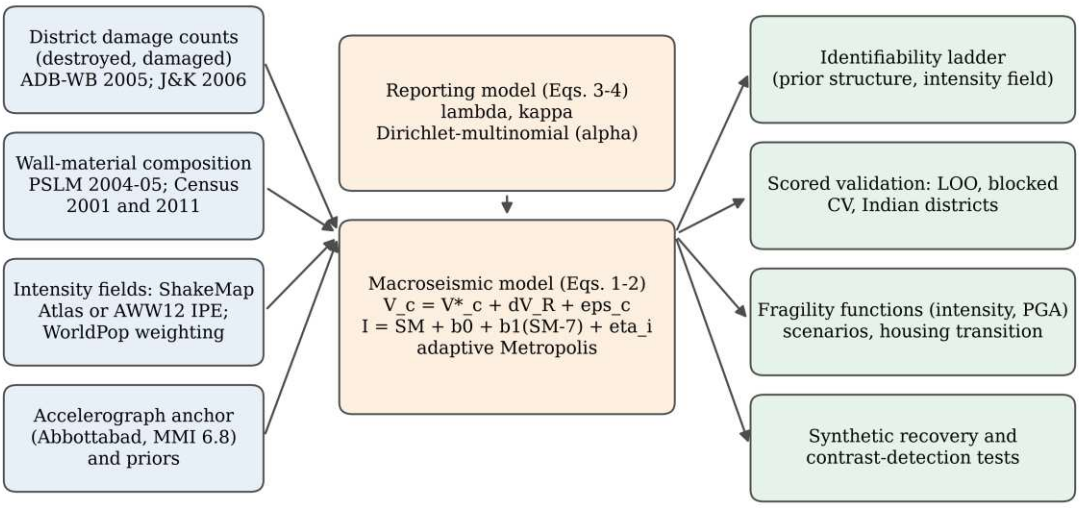


Fig. 3 Framework of the study

2.4.1 Reported categories and damage grades

For a building class c with vulnerability index V_c at intensity I, Eqs. (1) and (2) give the probabilities p_k of the EMS-98 damage grades. A threshold of "damage in excess of 40%" does not coincide with a damage grade. The probabilities that a dwelling is reported as destroyed or as damaged are therefore modeled as

$$P_{\text{destroyed}} = p_4 + p_5 + \lambda\, p_3 \tag{3}$$

$$P_{\text{damaged}} = p_2 + (1-\lambda)\, p_3 + \kappa\, p_1 \tag{4}$$

where $\lambda \in [0,1]$ is the share of grade-3 dwellings classified as destroyed and $\kappa \in [0,1]$ is the share of slightly damaged dwellings that were reported. The remainder are unreported or undamaged.

2.4.2 Hierarchical model

The vulnerability index of class c is written as

$$V_c = V_c^* + \Delta V_R + \varepsilon_c \tag{5}$$

Here V_c^* is the representative value of Table 2 (for brick and block masonry the mean of typologies M5, 0.74, and M6, 0.616; for timber-framed walls with infill typology M7, their closest mechanical analogue), ΔV_R (standard deviation 0.15) is a regional modifier common to all classes, and ε_c (standard deviation 0.08) is a class-specific

deviation, comparable to the half-width of the probable ranges of Lagomarsino and Giovinazzi (2006). All normal priors below are written as mean and standard deviation, and the notation is summarized in Table A1.

The true intensity in population cell j of district i is related to its ShakeMap value SM_{ij} by

$$I_{ij} = \mathrm{SM}_{ij} + b_0 + b_1\big(\mathrm{SM}_{ij} - 7\big) + \eta_i \qquad (6)$$

where $b_0 \sim N(0,\ 0.5)$ is a common bias of the ShakeMap level and $b_1 \sim N(0,\ 0.25)$ a slope bias. A positive b_1 means that ShakeMap is too flat, under-estimating strong and over-estimating weak shaking. The district deviation is $\eta_i \sim N(0,\ s_i)$, with s_i the population-weighted ShakeMap standard deviation (Table 3). In alternative forms the slope term is replaced by a distance term $b_1(R_i - 50)/50$, with R_i the rupture distance in km, or by a terrain term (Sect. 2.4.4). The probability that a dwelling of district i falls in reporting category r is the population- and composition-weighted average

$$P_{i,r} = \sum_j w_{ij} \sum_c m_{ic}\ P_r\big(I_{ij}, V_c\big) \qquad (7)$$

where w_{ij} is the population share of cell j (grouped in bins of 0.1 MMI), m_{ic} the share of class c, and P_r is given by Eqs. (3) and (4). The Abbottabad anchor adds the term $N(6.8 \mid I_{\mathrm{HQ}},\ 0.8)$, where I_{HQ} is the true intensity at the headquarters from Eq. (6). The reporting parameters have priors $\lambda \sim \mathrm{Beta}(2,2)$ and $\kappa \sim U(0,1)$. Eqs. (3)–(7) form model B, the reference model of this study. The earlier formulation (model A), which used the headquarters value as the only intensity of each district, no structured bias and the two Muzaffarabad estimates as constraints, is retained for comparison.

2.4.3 Likelihood and inference

The counts of destroyed, damaged and remaining dwellings in each district follow a Dirichlet-multinomial distribution. Its mean is given by Eq. (7), and its concentration parameter α ($\log\alpha \sim N(\log 100,\ 1.5)$) absorbs district-level variation not explained by intensity and composition. This is the between-unit variability that Ioannou et al. (2020) found must be modeled explicitly. Without this term, the likelihood of 787,583 dwellings would treat each district as an essentially exact measurement. The 18 parameters (ΔV_R, λ, κ, α, b_0, b_1, eight district deviations and four class deviations) were sampled with an adaptive Metropolis algorithm (Haario et al. 2001). Each chain ran 90,000 iterations, of which 30,000 were discarded as burn-in. Convergence was assessed with the Gelman–Rubin statistic of three independent chains (Gelman and Rubin 1992) and with batch-means effective sample sizes. The sampler bounds ($|\Delta V_R| < 0.6$, $|b_0| < 3$, $|b_1| < 1.5$, $|\eta_i| < 5$) are far outside the posterior mass. With 18 parameters and 16 informative fractions the model is nominally close to saturation; its effective number of parameters was therefore estimated with the widely applicable information criterion (Vehtari et al. 2017). Model B was developed after model A on the same eight districts. Both are reported, and the out-of-sample tests of Sects. 3.5 and 3.8 should be read with this specification history in mind.

2.4.4 Identifiability analysis

Three sources of information can separate intensity from vulnerability in Eq. (1). The first is the variation of wall composition between districts. The second is the intensity anchor. The third is the priors. The identifiability analysis compares the prior and posterior standard deviation of every parameter and of the contrasts between classes. It then refits the model with each source switched off or altered: no anchor; no structured bias; the

ShakeMap level fixed at −0.5 and +0.5 intensity units; a doubled ShakeMap uncertainty; class deviations with standard deviation 0.04 and 0.16; a regional modifier with standard deviation 0.30; the distance form of the bias; and a terrain form, in which the slope term is replaced by $b_1 z_i$, with z_i the standardized population-weighted slope-based V_{S30} of district i and $b_1 \sim N(0,\ 0.5)$, fitted with both priors. The composition and damage-model sensitivity cases of the earlier analysis are repeated: alternative AJK compositions, reassignment of 20%, 40% and 50% of "other" walls to brick and block, $V^*_{\text{stone}} = 0.74$, and the beta damage distribution. Further cases draw the compositions from Dirichlet distributions (concentration 300 for the surveyed districts, 20 for the assumed AJK composition), reclassify 77% of each district's destroyed and damaged dwellings as destroyed, the proportion of the later eligibility survey of the Earthquake Reconstruction and Rehabilitation Authority (ERRA) (Arshad and Athar 2013), and set Q to 2.0 and 2.6.

The typology-centered prior of Table 2 already encodes the expected ordering of the classes. Two tests therefore remove that information. In the first, the neutral prior, all classes receive the same prior center ($V_c^* = 0.71$, the mean of the four reference values) with class deviations of standard deviation 0.2 or 0.3, and any contrast in the posterior can therefore only come from the data. In the second, the ShakeMap prior is replaced by an intensity field that uses no damage observations (the damage-free field, AWW12), the intensity prediction equation of Allen et al. (2012) for active crustal regions:

$$I = c_0 + c_1 M + c_2 \ln\sqrt{R^2 + (1 + c_3 e^{\,M-5})^2} \tag{8}$$

with $M = 7.6$, R the rupture distance of each population cell (Sect. 2.3.4), $c_0 = 3.950$, $c_1 = 0.913$, $c_2 = -1.107$, $c_3 = 0.813$, and standard deviation $0.72 + 0.23/[1 + (R/44.7)^2]$, as implemented in the OpenQuake engine. Site amplification is neglected, as in the equation.

2.4.5 Scored validation

In leave-one-district-out validation, each district is withheld in turn and its destroyed and damaged fractions are predicted from the other seven. The intensity of the withheld district is known only from its ShakeMap distribution and a fresh deviation η. Predictions include the Dirichlet-multinomial overdispersion to describe an observed district fraction. They are scored with the continuous ranked probability score (Gneiting and Raftery 2007)

$$\text{CRPS}(F, y) = \text{E}_F|X - y| - 1/2\ \text{E}_F|X - X'| \tag{9}$$

where X and X' are independent draws from the predictive distribution F and y is the observed fraction. Lower values are better, and for a deterministic prediction the CRPS reduces to the absolute error.

Seven predictors are compared. Two deterministic mappings use the reference indices V^* with the population-weighted ShakeMap intensity taken as exact. The *standard mapping* counts grades 4–5 as "destroyed" and grades 2–3 as "damaged". The *grade-3 mapping* counts grades 3–5 as "destroyed", the natural reading of "damage in excess of 40%", and grades 1–2 as "damaged". *Climatology* uses the observed fractions of the other seven districts as the predictive ensemble. The *prior predictive* is model B with every parameter drawn from its prior. The *single-V* model is model B with one vulnerability index for all classes, which tests whether composition helps prediction at all. Models A and B are fitted on seven districts. For each predictor the mean CRPS, the mean width of the 90% interval and its coverage are reported. Differences from model B are given with 95% bootstrap intervals over districts and the number of districts in which model B scores better. Blocked cross-validation fits model B on the five Khyber Pakhtunkhwa districts and predicts the three AJK districts, and vice versa.

2.4.6 Synthetic recovery and value of finer data

Synthetic damage counts were generated from model B with known parameters (the posterior medians of the reference fit, $b_1 = 0$, $\alpha = 16$). They use the real population-weighted intensity distributions, compositions, dwelling totals and anchor, and were refitted with the same model. With 8 units the synthetic data mimic the real districts. With 16 and 32 units, each district is split into two or four sub-units, mimicking the release of tehsil or union-council records. The sub-units divide the dwellings equally, take compositions drawn from a Dirichlet distribution with concentration 30 around the district composition, and have intensity distributions shifted by an offset with standard deviation 0.3. Eight replicates were generated for each number of units. Two variants test this design: sub-unit compositions drawn with a concentration of 4, which makes the sub-units of a district differ strongly, and eight units with the intensity standard deviation of every district halved in both simulation and fit, which stands for better intensity information. The bias, the coverage of the 90% interval and the interval width were recorded. Since these tests use the posterior medians as truth, a second set avoids this inverse crime. Data were simulated with true stone–brick contrasts of 0 and 0.5 (brick 0.70, stone 0.70 or 1.20) and fitted with the exchangeable prior (class SD 0.3), with 8 and 32 units and three replicates each. These tests show whether the model detects a contrast that exists and avoids one that does not. A calibration study then quantifies the evidence carried by a given posterior probability at eight districts. One hundred data sets were simulated with true contrasts of 0 and 0.3, with district intensity deviations drawn independently of composition. A further 100 data sets with no contrast were simulated with deviations correlated with the stone share of each district ($r = 0.63$, the rank correlation between the posterior deviations and the stone share of the real data, Sect. 3.4). This misspecification test shows whether intensity errors aligned with composition can produce a spurious contrast. For each scenario, the share of data sets with a posterior probability of a positive contrast above 0.93 is reported with a Wilson 95% interval.

2.4.7 Fragility functions, transfer, joint calibration and scenarios

For each posterior draw and class, the exceedance probabilities $P(D \geq D_k \mid I)$ were computed from Eqs. (1) and (2) and fitted with a normal cumulative distribution in intensity, $P = \Phi[(I - \theta_k)/\sigma_k]$.

For the out-of-sample test in Indian Jammu and Kashmir, model B, calibrated on the Pakistani districts only, predicts the fully, partially and totally damaged houses of Baramulla, Kupwara and Punch (J&K). Every census unit receives its population-weighted ShakeMap distribution, the posterior bias terms and a fresh deviation η, and district predictions sum the units. The predictions are scored as in Sect. 2.4.5 against the standard mapping and the prior predictive. In a second step (model C), the three districts are added to the calibration. Each district shares one deviation η among its census units. Since the Indian relief survey used its own categories, it has its own reporting parameters $\lambda_{\mathrm{IN}} \sim \mathrm{Beta}(2,2)$ and $\kappa_{\mathrm{IN}} \sim U(0,1)$. Punch enters through its total only (beta-binomial). Model C was sampled as three independent chains, as model B.

Expected losses in Kashmir division were computed with model C for uniform scenario intensities VII, VIII and IX; intensity IX or above is associated with Zone V of the Indian seismic code IS 1893 (EERI 2005). The effect of the change in housing stock between 2001 and 2011 is expressed as the share of households reaching grade 4 or more, $P(D \geq D_4)$, at the same intensities, for the 2001 and 2011 compositions. A third composition moves all timber-walled households of 2011 to the brick and block class.

Lagomarsino and Giovinazzi (2006, Eqs. 24–25) relate V and Q to the yield spectral acceleration a_y, period T and ductility μ of a bilinear capacity curve. They assume the intensity–PGA correlation $a_g = c_1 c_2^{(I-5)}$ with $c_1 = 0.03$ g and $c_2 = 1.6$, and a Eurocode 8 (EC8) spectral shape. For $T < T_C$,

$$6.25\,V = 8.1 - 0.95\,Q - \log_{c_2}\left(\frac{a_y}{1.43 \times 2.5\,S\,c_1}\right) \qquad (10)$$

with $S = 1$ and $T_C = 0.4$ s. Applied to the parameters tabulated by Lagomarsino and Giovinazzi (2006, Table 5), this form reproduces their yield accelerations, for example 0.170 against 0.168 for typology M1_L and 0.142 for M3_H. Eq. (10) is applied with $Q = 2.3$ to the capacity of single-story dhajji-dewari measured on the shake table (Ali et al. 2017). The value of Q derived from the measured ductility is used as a sensitivity case. Lagomarsino and Giovinazzi (2006) note that this correspondence holds only for the intensity–acceleration correlation assumed. The anchor of Sect. 2.3.2 uses a different correlation (Wald et al. 1999), which corresponds to $c_1 = 0.067$ g and $c_2 = 1.876$ in Eq. (10). Both are therefore applied.

2.5 Use of AI tools

Large language model tools (Claude, Anthropic) were used to assist with writing and running the Python analysis code, searching and checking the literature, and drafting and editing the text. The code, results, references and text were checked, and full responsibility for the content of this article rests with the author.

3 Results and discussion

3.1 Consistency of ShakeMap intensities with the reported damage

When the ShakeMap Atlas intensities at the headquarters are treated as exact and a single vulnerability index is fitted to the destroyed and damaged counts, the fit is poor for every choice of intensity summary and damage-grade correspondence. The root-mean-square error of the destroyed fraction is 0.24–0.35, and the fitted index varies from 0.57 to 0.99. The observed pattern is not monotonic in ShakeMap intensity. Shangla lost 23% of its dwellings at MMI 5.6 and Batagram 64% at 7.6, whereas Abbottabad lost only 5% at 6.7.

The intensity implied by the observed damage, computed for a fixed vulnerability ($V = 0.74$, the simple-stone typology M3), makes the inconsistency explicit. For Muzaffarabad the destroyed fraction implies intensity 9.5 and for Abbottabad 7.7. For Bagh, Batagram and Shangla it implies 9.6, 9.8 and 8.6, about 2–3 degrees above their ShakeMap values. The destroyed fraction also implies systematically higher intensities than the any-damage fraction, by 1.5–2.8 degrees. This indicates that the "destroyed" category extends into EMS-98 grade 3, and it motivates the reporting parameters of Eqs. (3) and (4).

3.2 Joint posterior

The model converged (Gelman–Rubin statistic ≤ 1.002 for all parameters; effective sample sizes 740–1,020 for V_{stone}, b_0, b_1 and λ). Its effective number of parameters is 5.8, against 18 nominal parameters, with district contributions of 0.4–1.2; the model is therefore well below saturation. The posterior estimates are summarized in Table 4 and the posterior predictive fit in Fig. 4. The fit itself is not evidence for the model: with one deviation per district, the destroyed fractions are reproduced closely (root-mean-square error 0.065). The damaged fractions are

reproduced less well. Poonch (AJK) reported 63% of its dwellings damaged against a predicted 37%, and the "damaged" predictions vary little between districts, since the reporting parameter κ is common to all districts.

The vulnerability index of rubble-stone masonry is 0.96 (90% interval 0.81–1.10), and the probability that it exceeds the M1 representative value of 0.873 is 0.82. Its upper tail extends beyond the conventional upper limit of 1.02 of the macroseismic scale, the range that Lagomarsino and Giovinazzi (2006) reserve for behavior worse than vulnerability class A. Brick and block masonry is 0.68 (0.50–0.84). Table 4 lists the ratio of posterior to prior standard deviation; the prior standard deviation of each class index combines the regional modifier and the class deviation, and that of each contrast combines two class deviations. The data inform the stone index (ratio 0.52), the regional modifier (0.58), brick (0.60) and the reporting share of slight damage κ (0.49), which is pushed toward low values. They inform mud, timber and λ less (0.66–0.74) and the bias terms only marginally (0.84–0.92).

The contrasts between classes are informed least. The stone–brick contrast, 0.28 (0.12–0.44), has a posterior-to-prior ratio of 0.88, and the other contrasts 0.97–1.00. The typology-centered prior already gives the stone–brick contrast a probability of 0.958 of being positive, against 0.995 in the posterior. Whether the data themselves support a contrast is tested in Sect. 3.3. About two-thirds of grade-3 dwellings were classed as destroyed ($\lambda = 0.68$; 0.36–0.90), and only a small share of slightly damaged dwellings were reported ($\kappa = 0.14$; 0.01–0.44). The concentration $\alpha = 15$ indicates strong district-level overdispersion: the effective information content of each district is equivalent to some tens of dwellings rather than tens of thousands.

Table 4 Posterior summary of model B

Parameter	Median	90% interval	Prior SD	Posterior/prior SD
V, rubble stone	0.955	0.810 to 1.104	0.170	0.52
V, brick/block URM	0.677	0.498 to 0.842	0.170	0.60
V, mud/adobe	0.876	0.685 to 1.059	0.170	0.66
V, timber-framed	0.475	0.282 to 0.677	0.170	0.69
ΔV_R (regional modifier)	0.032	−0.109 to 0.177	0.150	0.58
$V_{\text{stone}} - V_{\text{brick}}$	0.282	0.122 to 0.442	0.113	0.88
$V_{\text{mud}} - V_{\text{brick}}$	0.201	0.012 to 0.385	0.113	1.00
$V_{\text{brick}} - V_{\text{timber}}$	0.196	0.026 to 0.384	0.113	0.97
λ (grade-3 share reported destroyed)	0.675	0.361 to 0.899	0.224	0.74
κ (grade-1 share reported damaged)	0.140	0.012 to 0.436	0.289	0.49
α (Dirichlet-multinomial concentration)	15.3	7.6 to 28.1	–	–
b_0 (ShakeMap level bias)	0.27	−0.45 to 0.94	0.50	0.84
b_1 (ShakeMap slope bias)	0.06	−0.32 to 0.44	0.25	0.92

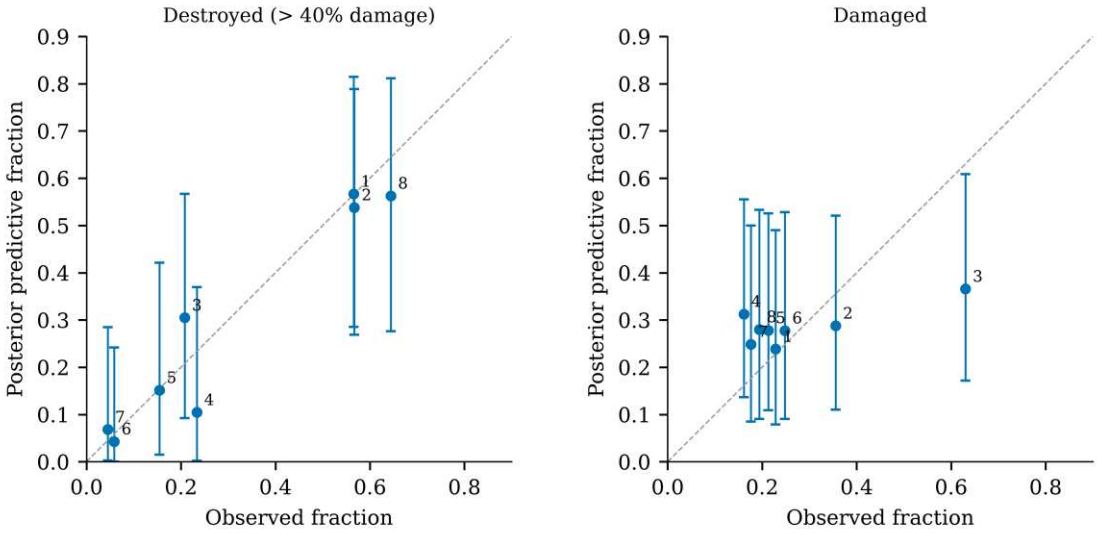


Fig. 4 Observed and posterior-predictive fractions of destroyed and damaged dwellings, model B. Districts: 1 Muzaffarabad, 2 Bagh, 3 Poonch (AJK), 4 Shangla, 5 Mansehra, 6 Kohistan, 7 Abbottabad, 8 Batagram

3.3 Identifiability of intensity and vulnerability

The results form a ladder of identifiability (Table 5, Fig. 5). Table 5 gives the contrast with its interval where posterior samples were retained and as a difference of medians otherwise, together with the root-mean-square error (RMSE) of the destroyed fraction; the cases share one random seed, different from that of Table 4, and small differences in the reference case are Monte Carlo error. In Fig. 5, the neutral-prior and damage-free cases are shown in orange, the gray band marks the probable range of typology M1, and the dashed line marks the difference of the representative values (0.195). At the bottom, each district's damage fixes a combination of its intensity and the vulnerability of its stock. The stone index and the ShakeMap level are therefore correlated in the posterior ($r = -0.67$, Fig. 5a). Fixing the ShakeMap level 0.5 units lower or higher moves the stone index to 1.05 or 0.92, about 0.065 per half degree, close to the 0.08 that a pure trade-off would give.

Given an intensity field, however, the stone index is determined by the data. With all classes centered on the same prior value of 0.71, it is still pulled to 0.96 (0.76–1.13) and 0.98 (0.78–1.16) for class deviations of SD 0.2 and 0.3. Replacing the ShakeMap prior by the damage-free field of Allen et al. (2012) gives 0.92 (0.78–1.06) with the typology-centered prior and 0.93 (0.71–1.11) with the neutral one. Across all 32 cases of Table 5 the stone index stays between 0.88 and 1.05. It falls below the M1 representative value only when its own reference is lowered to the simple-stone value of 0.74, and even there it rises from that reference by 0.14. Treating 77% of the damage as "destroyed", as in the later ERRA survey, raises it to 1.04, and reassigning 40% or 50% of the "other" walls to brick and block raises it to 1.01–1.02.

The next rung is the sign of the stone–brick contrast. From the neutral prior, where the contrast has probability 0.5 of being positive, the posterior probability rises to 0.93 and 0.96 (contrast 0.32 and 0.39; posterior-to-prior SD ratios 0.68 and 0.51), and to 0.94 with the damage-free field. When the slope term of the bias is replaced by a terrain term (Sect. 3.4), it falls to 0.86 and 0.90, whereas the stone index remains at 0.93–0.95. The data therefore lean toward a higher vulnerability of rubble stone than of brick and block masonry; however, the contrast is not established, since intensity errors that follow terrain or composition can produce it (Sect. 3.6), and its size is not resolved. The 90% intervals from the neutral prior span from about zero to 0.6–0.7, and the typology-centered

interval (0.12–0.44) is narrowed mainly by its prior. With the typology-centered prior the contrast is stable across the composition draws (0.23–0.29) and the other sensitivity cases, including the terrain term (0.27).

The top rung is not reached. From the neutral prior, the mud–brick, stone–timber and brick–timber contrasts have probabilities of 0.70–0.72, 0.72–0.79 and 0.32–0.35 of being positive. The data cannot order these classes, and the reference values of mud and timber are carried by their priors. Specifically, the data do not show timber-walled dwellings to be less vulnerable than brick ones. Their posterior-to-prior ratios of 0.66 for mud and 0.69 for timber (Table 4) show that the data narrow these indices only slightly, and the fragility functions of the two classes in Table 8 and Fig. 9 therefore reflect mainly the typology values on which their priors are centered.

Table 5 Identifiability and sensitivity cases (the composition-uncertainty row summarizes four Dirichlet draws)

Case	V **stone**	V **brick**	$V_{\text{stone}} - V_{\text{brick}}$	P**(contrast > 0)**	b_0	**RMSE**
Reference (model B)	0.95 (0.81–1.10)	0.68 (0.50–0.84)	0.28 (0.12–0.44)	0.995	0.27 (−0.45 to 0.93)	0.065
Prior structure and intensity field						
Neutral prior, class SD 0.2	0.96 (0.76–1.13)	0.65 (0.39–0.90)	0.32 (−0.04 to 0.60)	0.934	–	–
Neutral prior, class SD 0.3	0.98 (0.78–1.16)	0.59 (0.27–0.87)	0.39 (0.02–0.74)	0.958	–	–
Damage-free field (AWW12), typology-centered prior	0.92 (0.78–1.06)	0.64 (0.47–0.79)	0.29 (0.11–0.44)	0.995	0.19 (−0.49 to 0.88)	0.069
Damage-free field (AWW12), neutral prior	0.93 (0.71–1.11)	0.57 (0.27–0.87)	0.37 (−0.04 to 0.70)	0.937	0.18 (−0.54 to 0.90)	0.072
Terrain term (V_{S30}), typology-centered prior	0.95 (0.80–1.09)	0.68 (0.51–0.84)	0.27 (0.10–0.43)	0.992	0.29 (−0.40 to 0.97)	–
Terrain term (V_{S30}), neutral prior, class SD 0.2	0.93 (0.72–1.11)	0.66 (0.39–0.97)	0.28 (−0.20 to 0.58)	0.858	0.36 (−0.34 to 1.05)	–
Terrain term (V_{S30}), neutral prior, class SD 0.3	0.95 (0.71–1.15)	0.62 (0.31–0.97)	0.34 (−0.16 to 0.68)	0.896	0.29 (−0.47 to 1.00)	–
Intensity information						
Muzaffarabad field estimates added	0.97 (0.84–1.09)	0.69 (0.53–0.83)	0.28	–	0.18 (−0.41 to 0.77)	0.066
No intensity anchor	0.99 (0.84–1.14)	0.70 (0.52–0.88)	0.29	–	0.10 (−0.64 to 0.81)	0.065
No structured bias ($b_0 = b_1 = 0$)	0.99 (0.88–1.10)	0.70 (0.56–0.84)	0.29	–	0 (fixed)	0.066
ShakeMap level −0.5 (b_0 fixed)	1.05 (0.94–1.15)	0.76 (0.62–0.90)	0.29	–	−0.5 (fixed)	0.071
ShakeMap level +0.5 (b_0 fixed)	0.92 (0.81–1.03)	0.64 (0.50–0.79)	0.28	–	0.5 (fixed)	0.066
Distance form of bias	0.95 (0.82–1.09)	0.67 (0.50–0.83)	0.28	–	0.27 (−0.41 to 0.94)	0.066
ShakeMap SD × 2	0.92 (0.77–1.07)	0.65 (0.47–0.82)	0.27	–	0.21 (−0.52 to 0.93)	0.059
Prior scales						
Class deviation SD 0.04	0.93 (0.80–1.05)	0.70 (0.57–0.84)	0.23	–	0.28 (−0.40 to 0.97)	0.067
Class deviation SD 0.16	0.98 (0.81–1.14)	0.63 (0.41–0.83)	0.35	–	0.22 (−0.45 to 0.90)	0.064
Regional modifier SD 0.30	0.96 (0.81–1.11)	0.68 (0.50–0.85)	0.28	–	0.24 (−0.48 to 0.94)	0.066
$V^*_{\text{stone}} = 0.74$ (M3)	0.88 (0.73–1.03)	0.72 (0.55–0.89)	0.16	–	0.38 (−0.33 to 1.06)	0.071
Exposure, categories and damage model						
AJK composition = Batagram	0.95 (0.82–1.10)	0.65 (0.48–0.80)	0.30	–	0.24 (−0.45 to 0.91)	0.067
AJK composition = Mansehra	0.96 (0.81–1.10)	0.72 (0.57–0.87)	0.24	–	0.32 (−0.34 to 1.00)	0.068
20% of "other" walls as brick	0.98 (0.83–1.13)	0.70 (0.54–0.85)	0.28	–	0.30 (−0.37 to 0.97)	0.068
40% of "other" walls as brick	1.01 (0.85–1.16)	0.72 (0.58–0.87)	0.29	–	0.34 (−0.33 to 1.01)	0.074
50% of "other" walls as brick	1.02 (0.84–1.17)	0.73 (0.59–0.87)	0.29	–	0.37 (−0.32 to 1.03)	0.075
Composition uncertainty (4 Dirichlet draws)	0.94–0.96	0.66–0.72	0.23–0.29	0.982–0.995	–	–
ERRA-type categories (77% destroyed)	1.04 (0.89–1.19)	0.66 (0.50–0.81)	0.39 (0.22–0.54)	0.999	–	–
$Q = 2.0$	0.96 (0.82–1.10)	0.69 (0.52–0.85)	0.28 (0.11–0.43)	0.994	–	–
$Q = 2.6$	0.95 (0.81–1.09)	0.66 (0.50–0.83)	0.29 (0.11–0.45)	0.996	–	–
Beta damage distribution	0.95 (0.81–1.10)	0.68 (0.51–0.83)	0.27	–	0.25 (−0.42 to 0.95)	0.067

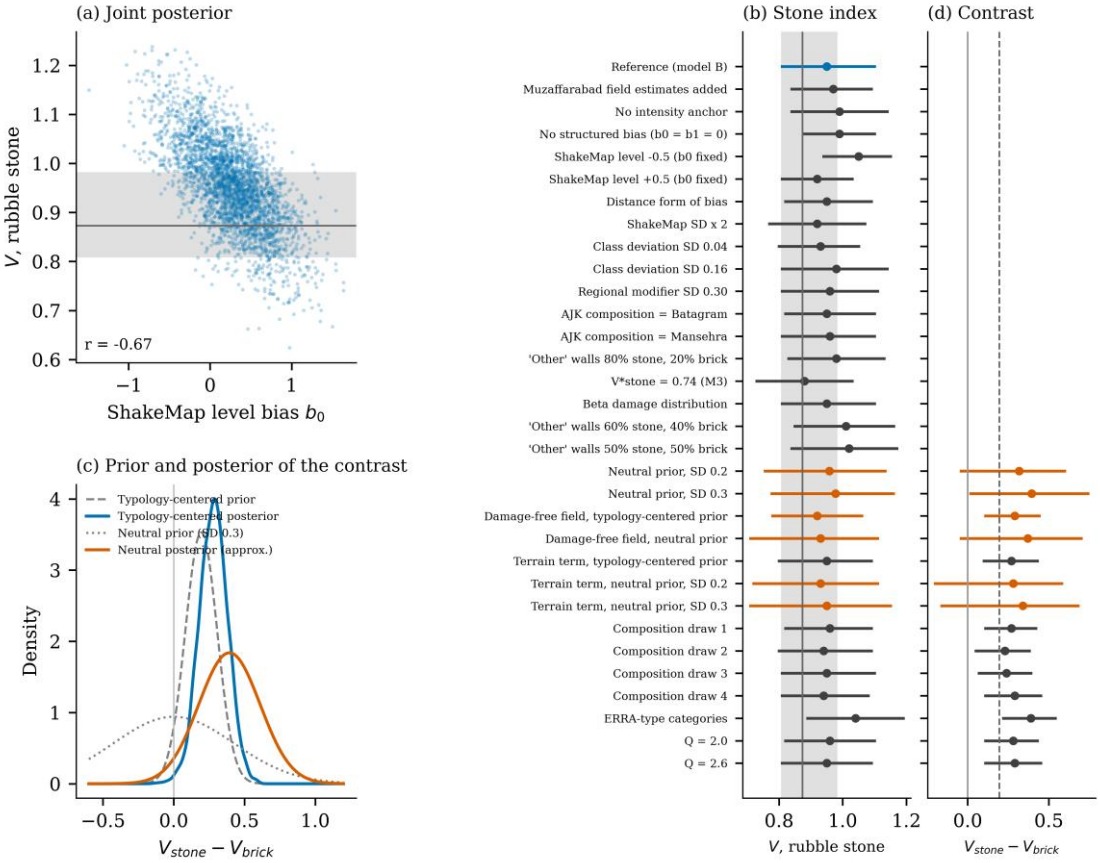


Fig. 5 Identifiability: (a) ShakeMap level bias and rubble-stone index, (b) rubble-stone index across the cases of Table 5, (c) prior and posterior densities of the stone–brick contrast, (d) stone–brick contrast across the cases of Table 5

3.4 Intensity bias and terrain effects

The data give no evidence of a structured ShakeMap bias. The slope term is $b_1 = 0.06$ (−0.32 to 0.44) and the distance term −0.03 (−0.43 to 0.38). Both posteriors are almost as wide as their priors (ratio 0.92). The level term $b_0 = 0.27$ (−0.45 to 0.94) is positive, although compatible with zero. The district deviations do not follow distance from the rupture (Fig. 6a). Bagh (16 km) and Batagram (32 km) are revised upwards by about 0.75 units, Mansehra (26 km) and Abbottabad (35 km) downwards by 0.65, and Shangla (62 km) and Kohistan (70 km) by less than 0.35 either way.

The deviations follow wall composition more closely (Fig. 6b; Spearman $\rho = 0.63$, $p = 0.09$). Part of the composition signal is therefore absorbed by the district intensities rather than by the class indices. This results from the tightly constrained class deviations and from the single composition shared by the three AJK districts. Composition is in turn correlated with terrain. The population-weighted, slope-based V_{S30} (time-averaged shear-wave velocity of the upper 30 m) of the ShakeMap grid is highest where rubble stone dominates ($\rho = 0.78$, $p = 0.02$), and the deviations follow it more weakly ($\rho = 0.43$, $p = 0.29$; Fig. 6c). Steep terrain favors both stone construction and the landsliding reported by EERI (2006). With eight districts, the effect of wall material cannot be separated from that of terrain and ground failure. This is the ecological-inference problem of inferring individual behavior from aggregates (Goodman 1953; King 1997), and the stone index should be read with it in mind. A refit in which the slope term of the bias is replaced by a terrain term $b_1 z_i$ tests this confounding directly (Table 5). The terrain coefficient is informed by the data ($b_1 = 0.29$–0.30, posterior-to-prior ratio 0.58–0.63), and the stone index is unchanged (0.93–0.95). From the neutral prior, the probability of a positive stone–brick contrast falls from 0.93–

0.96 to 0.86–0.90. The Abbottabad posterior (6.3; 90% interval 5.4–7.1) lies 0.5 units below the accelerograph value, within its uncertainty.

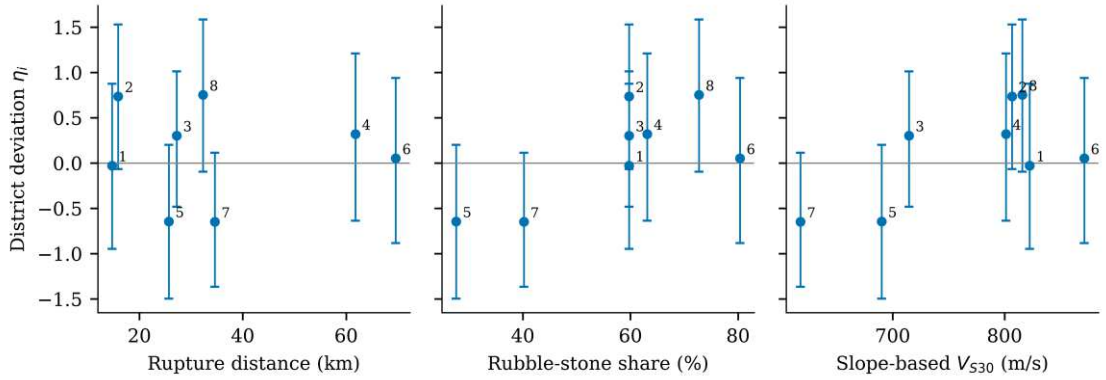


Fig. 6 Posterior district deviations against (a) rupture distance, (b) rubble-stone share and (c) slope-based V_{S30} (districts as in Fig. 4)

3.5 Scored validation

The robust predictive gain comes from modeling the reporting categories and the uncertainty of the intensity (Table 6, Fig. 7). The prior predictive, which calibrates nothing, scores better than both deterministic mappings in seven of eight districts. Against the standard mapping it reduces the mean CRPS of the destroyed fraction by 0.126 (95% bootstrap interval 0.048–0.203), and against the grade-3 mapping by 0.040 (0.007–0.076). Calibration then reduces the score further, by 0.025 for model B and 0.036 for model A. With eight districts this gain is not significant (model B: −0.009 to 0.059, better in six districts). Model A scores slightly better than model B in five districts, a difference of 0.011 (−0.015 to 0.036). Model B is retained as the reference for its physical basis, an intensity that describes the exposed population rather than one point (Sect. 2.3.4), and not for its predictive performance.

Composition matters for prediction. The class-structured model B scores better than the single-V model in seven of eight districts, by 0.027 (0.011–0.045). It also beats climatology, the spread of the other districts, in seven of eight, by 0.067 (0.034–0.101). For the damaged fraction, no probabilistic predictor is distinguishable from another; Poonch (AJK), with 63% of its dwellings reported damaged, is missed by all. The predictive intervals are wide, about 0.65 for the destroyed fraction, and all probabilistic predictors except climatology cover every withheld district. In blocked cross-validation, the five Khyber Pakhtunkhwa districts predict the three AJK districts and vice versa with a mean CRPS of 0.097, as in the leave-one-out case. All eight destroyed fractions, and six of eight damaged fractions, fall within the 90% intervals. Once vulnerability is calibrated, the uncertainty of a district loss estimate is dominated by the uncertainty of its intensity.

Table 6 Leave-one-district-out validation of the seven predictors

Predictor	CRPS destroyed	CRPS damaged	90% width destroyed	Coverage destroyed	Difference from model B, destroyed (95% CI)	Model B better
Standard mapping (D4–5)	0.247	0.156	0	0.00	0.151 (0.040 to 0.261)	6/8
Grade-3 mapping (D3–5)	0.161	0.254	0	0.00	0.065 (0.005 to 0.133)	6/8
Climatology	0.163	0.089	0.56	0.63	0.067 (0.034 to 0.101)	7/8
Prior predictive	0.121	0.089	0.66	1.00	0.025 (−0.009 to 0.059)	6/8
Single V (no class contrast)	0.123	0.083	0.66	1.00	0.027 (0.011 to 0.045)	7/8
Model A (headquarters intensity)	0.085	0.081	0.57	1.00	−0.011 (−0.036 to 0.015)	3/8
Model B	0.096	0.083	0.65	1.00	–	–

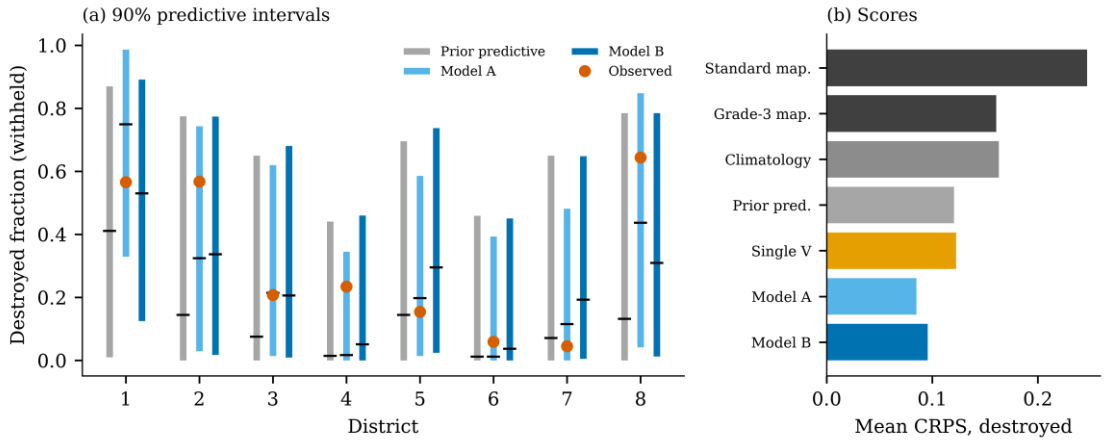


Fig. 7 Leave-one-district-out validation: (a) 90% predictive intervals of the destroyed fraction, (b) mean CRPS of the seven predictors

3.6 Synthetic recovery, contrast detection and value of finer data

The model recovers the parameters of synthetic data without material bias (Table 7). With eight units, the bias of the posterior median is 0.01 for the stone index and −0.02 for brick, and every 90% interval contains the true value. Coverage is 0.88–1.00 across parameters and numbers of units. Splitting the districts into 16 or 32 units, as tehsil or union-council records would allow, narrows the intervals less than might be expected (Fig. 8a). With four times as many units, the width of the stone interval decreases from 0.28 to 0.23 (18%), that of brick from 0.33 to 0.25 (23%) and that of λ from 0.61 to 0.41 (32%). The interval of the ShakeMap level b_0 changes only marginally (1.35 to 1.24). Each new unit brings its own intensity deviation, and the level is fixed only by the prior and the single anchor. This result does not depend on the similarity of the sub-units. With sub-unit compositions drawn with a concentration of 4, the stone interval narrows from 0.280 to 0.255 and 0.227 with 16 and 32 units, as in the reference design (Fig. 8a, dashed lines). Halving the intensity uncertainty of the eight districts narrows the stone interval only from 0.280 to 0.265 and that of b_0 by 2% (open symbols). Fixing the level itself narrows the real-data stone interval by about a quarter, from 0.29 to 0.21–0.22 (Table 5).

The contrast-detection tests do not use the posterior as truth (Fig. 8b, where dashed lines mark the true contrasts). For a true contrast of 0.5, the 90% interval excluded zero in five of six data sets, and the probability of a positive contrast was at least 0.94 in all six. For a true contrast of zero, five of six intervals contained zero. One data set with 32 units produced a spurious contrast of 0.30 (0.12–0.45), since its random intensity deviations happened to align with composition. With the neutral prior, the mean width of the 90% interval of the contrast decreases from 0.63 with eight units to 0.32 with 32 units, and all six intervals for the true contrast of 0.5 contain it, with medians of 0.37–0.58. Under the neutral prior, finer records therefore sharpen the contrast considerably. They do not protect it from aligned intensity deviations: the posterior probability of a positive contrast in the spurious case was 0.996, higher than the real-data values of 0.93–0.96 from the neutral prior; a high probability alone therefore does not distinguish a real contrast from aligned intensity errors.

A calibration study with 100 data sets per scenario at eight districts quantifies the evidence (Fig. 8c, where dashed lines mark the real-data probabilities and the outline the data sets with aligned intensity errors). With no contrast and independent intensity deviations, the posterior probability of a positive contrast exceeded 0.93 in 2 of 100 data sets (Wilson 95% interval 1–7%), and the 90% interval covered zero in 95. With a contrast of 0.3, the size estimated from the real data, the probability exceeded 0.93 in 29 of 100 data sets (21–39%). Probabilities as high as the real-data values of 0.93–0.96 are therefore about 15 times more likely under a contrast of this size than under

none (bootstrap 95% lower bound 5), and a contrast of 0.3 is missed more often than it is found. The misspecification test qualifies this result. With no contrast and intensity deviations aligned with the stone share (realized correlation 0.65), the probability exceeded 0.93 in 23 of 100 data sets (16–32%), with a median spurious contrast of 0.23 and a coverage of the 90% interval of 0.81. Intensity errors aligned with composition therefore produce a contrast of the real-data strength nearly as often as a true contrast of 0.3 does. The sign of the stone–brick contrast is therefore not established, since the aggregated data cannot verify that the district intensity errors are independent of wall composition.

Table 7 Synthetic recovery of the model parameters with the typology-centered prior

Parameter	Units	Bias	RMSE	90% coverage	Mean 90% width
V, rubble stone	8	0.012	0.045	1.00	0.28
	16	−0.002	0.037	1.00	0.26
	32	−0.015	0.044	1.00	0.23
V, brick/block	8	−0.020	0.067	1.00	0.33
	16	0.055	0.076	0.88	0.29
	32	0.024	0.062	0.88	0.25
V, mud/adobe	8	0.008	0.041	1.00	0.38
	16	0.022	0.036	1.00	0.35
	32	0.006	0.040	1.00	0.32
λ	8	−0.049	0.079	1.00	0.61
	16	−0.039	0.066	1.00	0.51
	32	0.002	0.058	1.00	0.41
b_0	8	−0.061	0.211	1.00	1.35
	16	−0.098	0.197	1.00	1.32
	32	−0.062	0.160	1.00	1.24

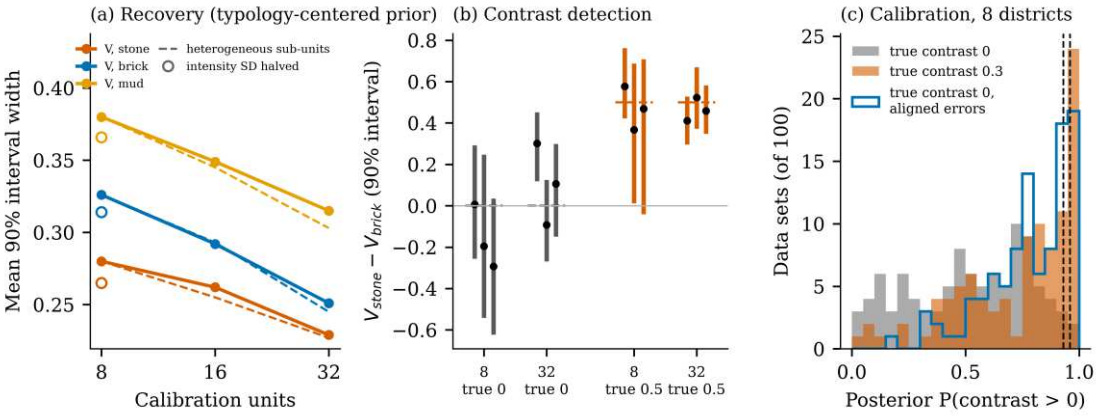


Fig. 8 Synthetic tests: (a) interval width against the number of calibration units, (b) contrast detection, (c) calibration of the contrast probability at eight districts

3.7 Fragility functions

Fragility parameters for the four wall classes are listed in Table 8 and plotted in Fig. 9. The median intensities θ_k were computed from a subsample of 400 posterior draws, σ_k is given as its range over classes, and values above intensity XII are extrapolations of Eq. (1). The median intensity for very heavy damage (grade 4) is 8.0 for rubble stone and 9.8 for brick masonry. The dispersion σ_k is about one intensity degree for grades 2–4 and larger for grades 1 and 5. It follows from the binomial damage distribution and the fixed ductility index, not from the data. The stone curves are the best constrained. The mud and timber-framed curves reflect mainly their priors (Sect. 3.3).

All curves shift together by about 0.4 degrees for each 0.5-degree change in the ShakeMap level, whereas the spacing between the stone and brick curves is not established by the data.

Table 8 Fragility parameters in intensity by wall class

	Rubble stone	**Mud/adobe**	**Brick/block URM**	**Timber-framed**	σ_k
V	0.96 (0.81–1.10)	0.88 (0.69–1.06)	0.68 (0.50–0.84)	0.48 (0.28–0.68)	
θ_1	4.8 (3.8–5.9)	5.4 (4.2–6.6)	6.6 (5.6–7.6)	7.8 (6.5–9.1)	1.40–1.46
θ_2	6.2 (5.1–7.2)	6.7 (5.5–8.0)	7.9 (7.0–9.0)	9.2 (7.9–10.5)	1.07
θ_3	7.1 (6.1–8.2)	7.7 (6.5–8.9)	8.9 (7.9–9.9)	10.1 (8.8–11.4)	1.00
θ_4	8.0 (7.0–9.1)	8.6 (7.4–9.9)	9.8 (8.8–10.8)	11.1 (9.7–12.3)	1.07
θ_5	9.4 (8.4–10.4)	9.9 (8.7–11.2)	11.1 (10.2–12.1)	12.3 (11.1–13.5)	1.28–1.46

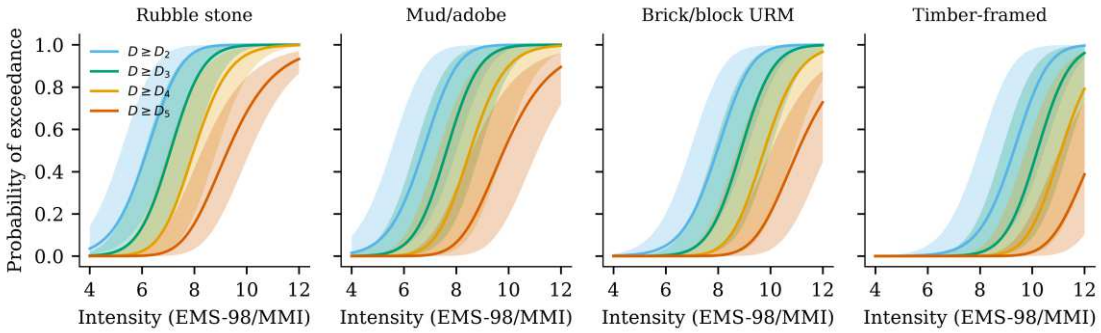


Fig. 9 Calibrated fragility functions by wall class, model B

For use in acceleration-based risk models, the medians were converted to peak ground acceleration (Table 9, Fig. 10). The 90% intervals of Table 9 follow from the intensity intervals, values above about 1.5 g are extrapolations, and the timber-framed class is omitted since its values are prior-dominated and largely extrapolated. The conversion dominates the result. The relation of Wald et al. (1999) gives medians three to six times higher than the correlation of Lagomarsino and Giovinazzi (2006) (L&G); for grade 4 of rubble stone they are 0.44 g and 0.12 g. The Nepalese stone-masonry medians of Gautam (2018), 0.09–0.42 g for grades 2–5, lie between the two conversions of the stone curves and close to the brick curve under the L&G correlation. The half-dressed stone model of Ahmad et al. (2012c) collapsed at a table acceleration of 0.20 g, close to the stone collapse median under the L&G correlation (0.24 g) and far below that under the Wald relation (1.07 g). Only the Wald relation is consistent with the intensity scale of the calibration. Under the L&G correlation, the Abbottabad acceleration of 0.213 g would correspond to intensity 9.2, against 6.8 under the Wald relation, 6.7 in the ShakeMap and a posterior of 6.3 (5.4–7.1). The L&G values are therefore given for comparison with the typology framework, in which that correlation is assumed. The PGA values should be used with the conversion stated, and the comparison argues for a regionally validated intensity–acceleration relation.

Table 9 Median peak ground acceleration (g) of the fragility functions under two intensity–acceleration conversions (Wald et al. 1999; Lagomarsino and Giovinazzi 2006)

Class	**Conversion**	D_2	D_3	D_4	D_5
Rubble stone	Wald et al. (1999)	0.14 (0.07–0.27)	0.25 (0.13–0.50)	0.44 (0.24–0.89)	1.07 (0.57–2.01)
Rubble stone	L&G (2006)	0.05 (0.03–0.08)	0.08 (0.05–0.13)	0.12 (0.08–0.21)	0.24 (0.15–0.38)
Mud/adobe	Wald et al. (1999)	0.20 (0.09–0.44)	0.37 (0.17–0.78)	0.65 (0.30–1.47)	1.47 (0.69–3.33)
Mud/adobe	L&G (2006)	0.07 (0.04–0.12)	0.11 (0.06–0.19)	0.16 (0.09–0.30)	0.30 (0.17–0.55)
Brick/block URM	Wald et al. (1999)	0.42 (0.24–0.83)	0.78 (0.42–1.47)	1.38 (0.73–2.59)	3.12 (1.77–5.86)
Brick/block URM	L&G (2006)	0.12 (0.08–0.20)	0.19 (0.12–0.30)	0.29 (0.18–0.46)	0.53 (0.35–0.84)

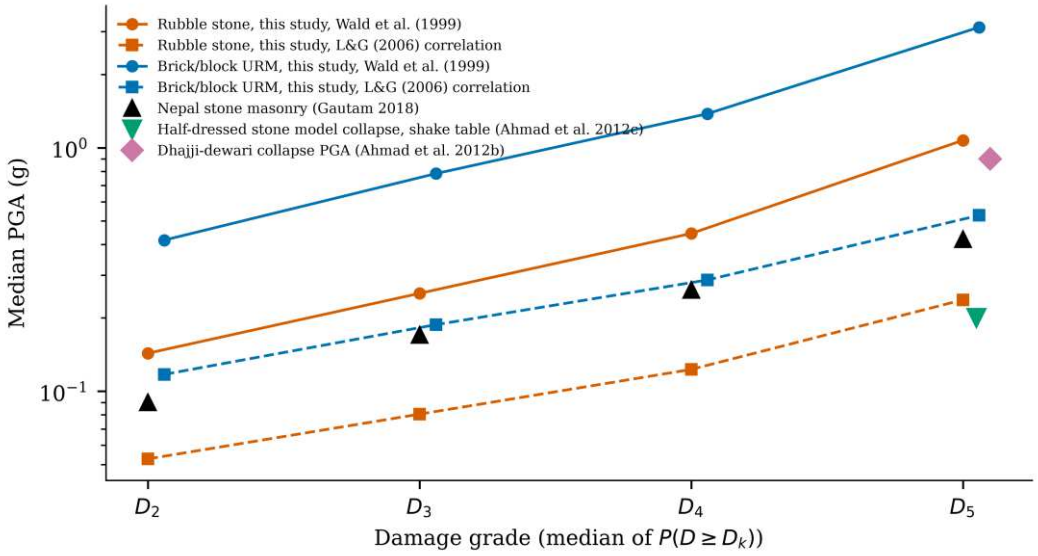


Fig. 10 Median PGA of the stone and brick fragility functions compared with published values (Gautam 2018; Ahmad et al. 2012c; Ahmad et al. 2012b)

3.8 Out-of-sample test in Indian Jammu and Kashmir

The census shows sharply contrasting exposure on the Indian side (Table 10). For Uri and Karnah, the intensities were taken within 15 km of Uri and 10 km of Tangdhar. The Line-of-Control tehsils Uri and Karnah, which suffered most, are more than 90% rubble stone, like the Pakistani hill districts. The valley districts of Srinagar, Badgam and Pulwama are dominated by burnt-brick construction. In the rest of Kupwara, almost half of the households live in timber-walled dwellings. Punch (J&K) and Rajouri in Jammu division are more than 80% rubble stone and lie 52 and 96 km from the rupture.

Table 10 Exposure units in Indian Jammu and Kashmir (ORGI 2001a; ORGI 2001b; ORGI 2001c; Rai and Murty 2006)

Unit	Households	Brick	Mud	Timber	Stone	Population-weighted MMI (SD)	Rupture distance (km)	Field
Uri tehsil	13,919	0.01	0.01	0.02	0.95	7.5 (0.80)	9	VIII
Rest of Baramulla	139,394	0.70	0.19	0.06	0.05	6.7 (0.89)	46	VII
Karnah tehsil	6,256	0.00	0.01	0.04	0.94	7.3 (0.92)	15	–
Rest of Kupwara	80,122	0.43	0.10	0.45	0.03	6.6 (0.94)	37	VII
Srinagar	162,254	0.78	0.14	0.05	0.03	5.7 (0.91)	78	V
Badgam	86,166	0.81	0.15	0.03	0.01	6.1 (0.93)	64	–
Pulwama	93,293	0.73	0.24	0.03	0.00	5.7 (0.94)	91	–
Anantnag	158,193	0.56	0.38	0.04	0.01	5.4 (0.93)	118	–
Punch	59,570	0.07	0.06	0.00	0.87	6.0 (0.91)	52	–
Rajouri	81,757	0.16	0.01	0.00	0.83	5.6 (0.91)	96	–

Calibrated on the Pakistani districts alone, model B predicts the final official counts of fully damaged houses within its 90% intervals in both districts for which they are reported (Table 11, Fig. 11). In Table 11, all counts are houses, Baramulla includes Uri and Kupwara includes Karnah. In Baramulla, which contains Uri, it predicts 18,400 (90% interval 3,600–72,500) fully damaged houses against about 15,000 reported. It also predicts 37,600 (9,600–73,500) partially damaged against 39,373, and 61,600 (17,600–126,100) in total against 54,373. In Kupwara it predicts 6,300 (1,100–31,600) fully damaged against 9,305. The standard mapping under-predicts the fully damaged houses by factors of 4.2 and 7.5. For the fully damaged fraction, model B reduces its mean CRPS from 0.084 to 0.028 and improves on the prior predictive (0.034).

The test also exposes clear failures. The partially damaged houses of Kupwara (55,076 reported) are under-predicted (15,100; 3,000–36,500), as is its total (64,381, outside the interval 6,400–60,100). The Punch (J&K) total (8,072) lies inside the interval, although it is over-predicted 3.6-fold (29,000; 4,900–55,800). Over the seven comparisons, model B scores better than the prior predictive in three and the standard mapping in five, and covers five. For partial and total damage, calibration on Pakistan does not improve on the prior predictive (mean CRPS 0.202 against 0.175 for partial damage and 0.203 against 0.184 for the totals). This is consistent with the more inclusive definition of partial damage suggested by the reported ratios (Sect. 2.3.5). The share of slightly damaged dwellings reported, κ, is learned from the Pakistani assessment and does not transfer. The failures may also reflect a different vulnerability of the timber-walled stock of Kupwara, which the data cannot resolve (Sect. 3.3).

Table 11 Out-of-sample prediction of the final official damage counts in Indian Jammu and Kashmir (UNI 2006)

District	Category	Reported	Model B, median (90%)	Standard mapping	Prior predictive, median (90%)
Baramulla	Fully damaged	15,000	18,400 (3,600–72,500)	3,600	10,900 (90–76,900)
Baramulla	Partially damaged	39,373	37,600 (9,600–73,500)	36,700	50,600 (9,100–91,300)
Baramulla	Total	54,373	61,600 (17,600–126,100)	40,300	66,200 (11,200–139,400)
Kupwara	Fully damaged	9,305	6,300 (1,100–31,600)	1,200	3,900 (20–30,700)
Kupwara	Partially damaged	55,076	15,100 (3,000–36,500)	13,300	20,900 (3,900–45,100)
Kupwara	Total	64,381	23,200 (6,400–60,100)	14,600	25,900 (5,000–69,400)
Punch (J&K)	Total	8,072	29,000 (4,900–55,800)	14,100	26,900 (2,400–57,000)

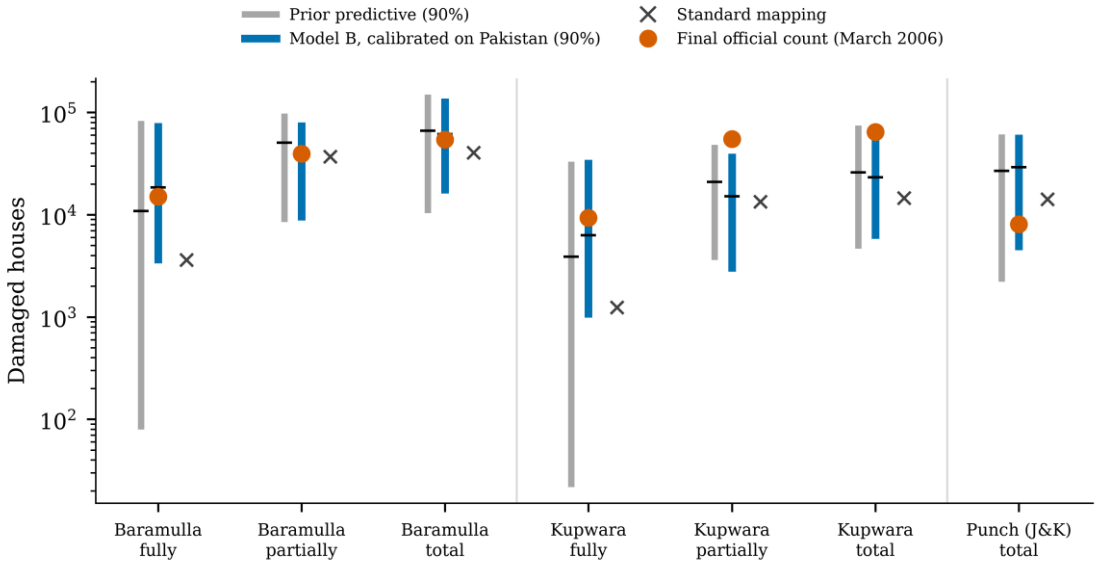


Fig. 11 Out-of-sample prediction of damaged houses in Baramulla, Kupwara and Punch (J&K) (UNI 2006)

3.9 Joint calibration on both sides of the Line of Control

Adding the three Indian districts to the calibration (model C; maximum $\hat{R}$ 1.003, effective sample sizes 2,600–3,100 for the class indices) leaves the vulnerability estimates nearly unchanged and narrows them slightly (Table 12). The stone index is 0.93 (0.79–1.07), the stone–brick contrast 0.27 (0.11–0.41), and the posterior-to-prior ratios of the class indices decrease by up to 0.06. With $\alpha \approx 14$, the three districts carry little weight, and the agreement of models B and C is consistency rather than independent confirmation. The Indian relief survey reported a larger share of slightly damaged houses than the Pakistani assessment ($\kappa_{\mathrm{IN}} = 0.45$ against $\kappa = 0.15$), although both are uncertain. The district deviations place Kupwara one intensity unit above its ShakeMap distribution (1.0; 0.1 to 1.9)

and Punch (J&K) 1.3 units below it (−2.3 to −0.3). Even with these terms the partially damaged houses of Kupwara are under-predicted (33,700 against 55,076).

Table 12 Vulnerability indices and reporting parameters of models B and C

Parameter	Model B (Pakistan)	Model C (Pakistan and India)
V, rubble stone	0.96 (0.81–1.10)	0.93 (0.79–1.07)
V, brick/block URM	0.68 (0.50–0.84)	0.67 (0.51–0.81)
V, mud/adobe	0.88 (0.69–1.06)	0.88 (0.69–1.06)
V, timber-framed	0.48 (0.28–0.68)	0.52 (0.33–0.70)
$V_{\text{stone}} - V_{\text{brick}}$	0.28 (0.12–0.44)	0.27 (0.11–0.41)
Posterior/prior SD, stone / brick / mud / timber	0.52 / 0.60 / 0.66 / 0.69	0.50 / 0.54 / 0.66 / 0.65
λ / κ, Pakistani assessment	0.68 / 0.14	0.67 / 0.15
λ_{IN} / κ_{IN}, Indian relief survey	–	0.45 / 0.45
η, Baramulla / Kupwara / Punch (J&K)	–	−0.21 / 1.02 / −1.29
Convergence: max $\hat{R}$; effective sample size	1.002; 740–1,020 (Sect. 3.2)	1.003; 2,600–3,100 (class indices)

3.10 Scenario for Kashmir division

Three damage measures are distinguished in this study. "Destroyed" is the reporting category of Eq. (3), which includes the share λ of grade-3 dwellings. $P(D \geq D_3)$ and $P(D \geq D_4)$ are the shares of dwellings reaching EMS-98 grade 3 (substantial to heavy damage) and grade 4 (very heavy damage) or more. For uniform intensities VII, VIII and IX, model C predicts that 7%, 22% and 50% of the 740,000 households of Kashmir division would be reported destroyed (Table 13). Table 13 uses the 2001 census stock, and its class columns give the share of each class reported destroyed. The corresponding shares reaching grade 3 are 10%, 29% and 59%, and grade 4, 3%, 11% and 31%. The shares reaching grade 4 are computed from the same posterior draws and composition as Table 15. At intensity IX, 90% of rubble-stone, 83% of mud, 41% of brick and 14% of timber-framed dwellings would be reported destroyed, the last two figures resting mainly on their priors. Most of the expected losses arise from the large brick and mud stock of the valley districts, whereas the highest proportional losses arise in the stone-built Line-of-Control tehsils. The scenario illustrates the calibrated functions, and its absolute level is conditional on the ShakeMap intensity level, as is that of the functions themselves.

Table 13 Expected damage in Kashmir division for uniform scenario intensities, model C

Intensity	Reported destroyed, households	Reported destroyed	$P(D \geq D_3)$	$P(D \geq D_4)$	Stone	Mud	Brick	Timber
VII	55,200 (13,800–143,600)	7%	10%	3%	31%	19 %	2%	0%
VIII	166,100 (63,100–331,700)	22%	29%	11%	67%	52 %	13%	2%
IX	366,400 (192,500–553,800)	50%	59%	31%	90%	83 %	41%	14%

3.11 Timber-reinforced construction and its replacement

3.11.1 Mechanical evidence for dhajji-dewari

The aggregated data cannot isolate taq and dhajji-dewari, since neither appears as a census category; the timber-framed class of Table 2 is defined by wall material and its index reflects its prior (Sect. 3.3). The vulnerability of dhajji-dewari was therefore derived independently from published shake-table data through Eq. (10). Ali et al. (2017) tested two single-story dhajji-dewari models. In Model 1, elastic behavior ended at a base shear coefficient of 0.52 (story drift 0.13%), maximum resistance was 0.69 at 0.74% drift, and the yield period was 0.16 s. In Model

2, the corresponding values were 0.45 (0.18%), 1.60 (1.28%) and 0.21 s. The base shear coefficient, normalized by the seismic weight, is taken as the yield spectral acceleration a_y; the idealized yield value lies between the elastic-limit and maximum-resistance values.

With the correlation of Lagomarsino and Giovinazzi (2006), Eq. (10) gives $V = 0.41$ and 0.46 for the two models at their elastic-limit strength, and lower values, down to 0.03, for higher idealized strengths (Table 14, Fig. 12). Table 14 uses $Q = 2.3$, and values of θ above XII under the L&G correlation are extrapolations of Eq. (1). With the correlation consistent with the anchor (Wald et al. 1999), the same capacities give 0.75 and 0.79 at the elastic limit and 0.47–0.71 for higher strengths. The difference arises from the Wald relation, which assigns a given intensity a peak acceleration roughly three times higher; the same capacity therefore corresponds to a lower intensity. Using Q derived from the measured ductility (1.2–2.8) changes V by less than 0.1 in most cases.

Table 14 Vulnerability index of single-story dhajji-dewari from shake-table capacity (Ali et al. 2017)

Model	a_y (g)	Basis	T (s)	V, L&G correlation	V, Wald-consistent	θ_4	θ_5
1	0.52	elastic limit	0.16	0.41	0.75	11.4	12.7
1	0.60	mid-range	0.16	0.36	0.71	11.8	13.1
1	0.69	maximum resistance	0.16	0.31	0.68	12.1	13.3
2	0.45	elastic limit	0.21	0.46	0.79	11.1	12.4
2	1.03	mid-range	0.21	0.18	0.58	12.9	14.2
2	1.60	maximum resistance	0.21	0.03	0.47	13.8	15.0

The mechanical evidence therefore places dhajji-dewari anywhere between 0.03 and 0.79, depending on the intensity–acceleration correlation and the idealized yield strength. Under the L&G correlation, it is less vulnerable than both rubble stone (0.96) and brick and block masonry (0.68). Under the Wald-consistent correlation it remains less vulnerable than rubble stone, by 0.17–0.49, and comparable to brick and block masonry. Which correlation applies to the region is not known (Sect. 3.7). The observation that timber-laced construction performed better than unreinforced masonry in 2005 (Rai and Murty 2006; Ahmad et al. 2017) is consistent with either. The collapse PGA of about 0.9 g estimated by Ahmad et al. (2012b) corresponds to intensity 12.2 under the L&G correlation and to 9.1 under the Wald relation.

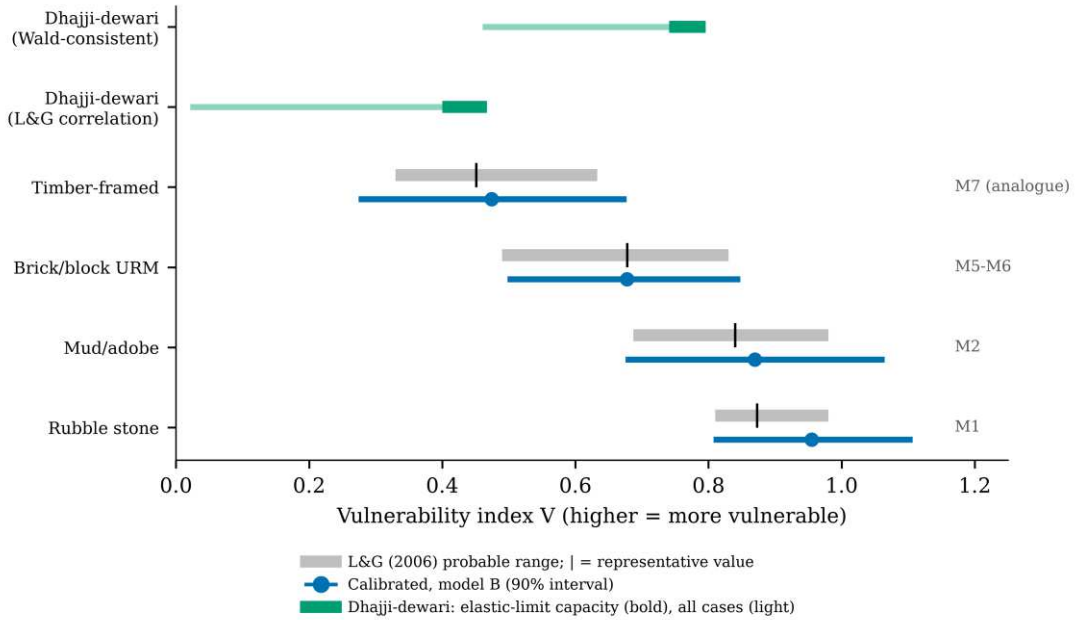


Fig. 12 Vulnerability index by wall class: typology ranges (Lagomarsino and Giovinazzi 2006), damage-calibrated values and mechanical estimates for dhajji-dewari (Ali et al. 2017)

These estimates refer to well-built laboratory specimens, and dwellings with decayed timber, missing braces or heavy roofs will be more vulnerable. The two-story structure of Ali et al. (2021) reached a yield base shear coefficient of 1.38 at 2.9% drift and an ultimate drift of 7.6%. This deformation capacity is consistent with low vulnerability; however, the period at yield required by Eq. (10) is not reported. For taq, no capacity curve, test or post-earthquake damage statistic is available; its mechanism has been described only qualitatively (Dhandapany and Menon 2019). Taq therefore cannot yet be placed on the vulnerability scale, and its quantification by testing or detailed modeling is the main gap left by this study.

3.11.2 Replacement of timber-walled dwellings, 2001–2011

Between the censuses of 2001 and 2011 the number of households in Kashmir division grew by 29%, and the share living in timber-walled dwellings fell from 8.7% to 5.8% (Table 15, Fig. 13a; 2001 district boundaries). The change is concentrated in Kupwara, the district where timber walls were most common. There, their share fell from 41.8% to 28.9%, and the number of timber-walled households declined in absolute terms, from 36,100 to 30,900, while brick and block walls rose from 39.6% to 48.6%. In the valley districts the dominant change was from mud to brick, for example in Anantnag from 37.9% to 26.0% mud walls.

These transitions have opposite effects on risk, and both depend on class contrasts that the damage data do not establish. Replacing mud by brick lowers the expected share of households reaching grade 4 or more, in line with the typology ordering of these two classes, whose contrast is prior-dominated. For Kashmir division as a whole the share at intensity VIII changes little (11.2% to 10.5%). The effect of replacing timber by brick depends entirely on the timber index, which the damage data do not identify. Fig. 13b shows the change in Kupwara for a range of assumed timber indices, with the other classes from the jointly calibrated posterior; shading marks the dhajji-dewari indices under the two correlations and the dashed line the calibrated brick index. The share reaching grade 4 at intensity VIII increases between 2001 and 2011 for any timber index below about 0.78, by about 1.7 percentage points (5–95%: 0.5–3.7) if the index is 0.5 or lower. The probability of an increase is at least 0.98 for indices up to 0.65 and 0.91 at 0.70, and falls below one half above 0.78.

The mechanical estimate for dhajji-dewari (Sect. 3.11.1) lies entirely below this break-even value under the L&G correlation and mostly below it under the Wald-consistent one, where the elastic-limit capacity reaches it. The current practice of brick or block masonry with reinforced-concrete floors corresponds to typology M6 ($V^* = 0.616$), and large openings would make it more vulnerable. Where it replaces well-built timber-braced construction, it is expected to raise risk; however, this conclusion rests on the mechanical evidence and on post-earthquake observations rather than on the damage statistics.

Table 15 Wall material of households in 2001 and 2011 and share reaching grade 4 at intensity VIII (ORGI 2001a; ORGI 2011)

Unit	Households 2001 / 2011	Timber (%) 2001 → 2011	Brick/block (%) 2001 → 2011	Mud (%) 2001 → 2011	$P(D \geq D_4)$ at VIII, 2001 stock	2011 stock	2011, timber replaced
Kupwara	86,400 / 106,800	41.8 → 28.9	39.6 → 48.6	9.4 → 12.3	8.8 (3.1–19.6)	10.4 (3.6–22.3)	11.3 (3.7–25.6)
Baramulla	153,300 / 202,800	5.4 → 5.6	64.0 → 65.1	17.2 → 17.9	13.8 (4.7–28.4)	13.3 (4.3–27.8)	13.5 (4.3–28.3)
Srinagar	162,300 / 210,700	4.7 → 2.7	77.8 → 83.5	14.2 → 9.2	8.9 (2.2–23.1)	8.0 (2.1–22.3)	8.1 (2.1–22.7)
Badgam	86,200 / 99,200	3.2 → 1.3	81.2 → 88.9	15.0 → 8.6	8.1 (1.6–22.6)	6.6 (1.2–20.6)	6.6 (1.2–20.8)
Pulwama	93,300 / 123,200	3.1 → 1.6	72.6 → 73.0	23.9 → 23.9	10.4 (1.8–27.1)	10.9 (2.2–27.3)	10.9 (2.2–27.5)
Anantnag	158,200 / 212,200	4.4 → 2.0	56.5 → 69.7	37.9 → 26.0	14.5 (2.7–33.6)	11.7 (2.6–28.9)	11.8 (2.6–29.1)
Kashmir division	739,600 / 954,900	8.7 → 5.8	65.7 → 71.8	20.7 → 17.0	11.2 (2.9–26.5)	10.5 (2.8–25.6)	10.7 (2.8–25.9)
Punch	59,600 / 88,900	0.1 → 0.3	6.6 → 12.0	6.0 → 3.1	39.4 (14.7–67.0)	37.5 (13.6–64.6)	37.5 (13.6–64.6)
Rajouri	81,800 / 124,000	0.2 → 0.4	16.2 → 24.2	1.1 → 2.3	36.0 (13.0–62.6)	33.0 (12.0–56.8)	33.0 (12.0–56.8)

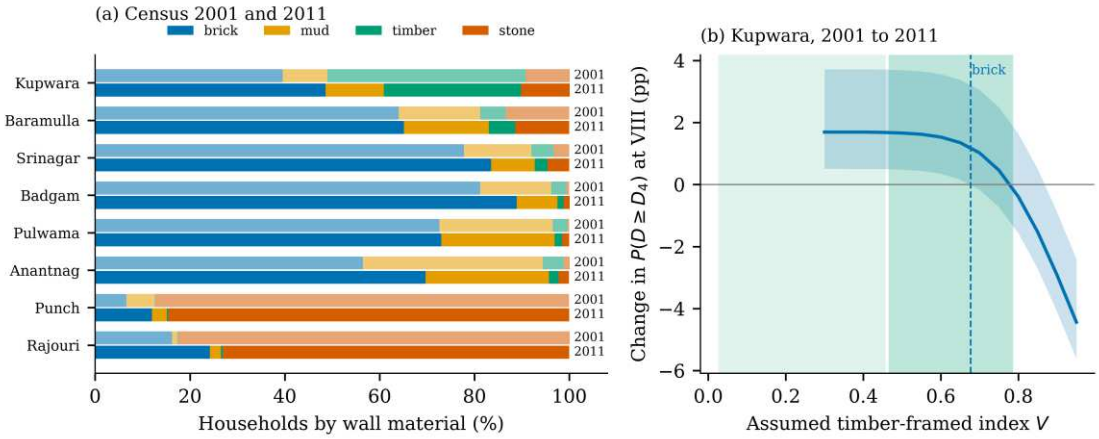


Fig. 13 Housing transition in Indian Jammu and Kashmir: (a) households by wall material in 2001 and 2011 (ORGI 2001a; ORGI 2011), (b) change in the Kupwara share reaching grade 4 at intensity VIII against the assumed timber index

3.12 Vulnerability of Himalayan stone masonry

The calibrated index of rubble-stone masonry (0.96) lies near the upper bound of the probable range of the reference typology, and implies that very heavy damage becomes the median outcome at intensity VIII. It is the quantity best constrained by the data, and it holds under neutral priors, a damage-free intensity field and a terrain term in the intensity bias. It agrees with independent lines of evidence. Reconnaissance teams observed that random-rubble stone walls "collapsed at levels of much lesser shaking" than other construction (EERI 2005). They attributed the destruction to the lack of integrity of masonry built in mud or lean mortar, and to heavy roofs (Bothara and Hiçyılmaz 2008; Naseer et al. 2010). Maqsood and Schwarz (2008) assigned the regional stock to lower vulnerability classes than is typical. The same authors report that almost half of the brick masonry dwellings with reinforced-concrete slabs were severely damaged in the areas they visited (intensity IX–X), and almost 95% of adobe dwellings heavily damaged. At intensity IX, the calibrated functions give 55% of brick and 91% of mud dwellings at grade 3 or above. Shake-table tests on regional rubble-stone models showed damage and collapse at low input accelerations (Ali et al. 2013; Ahmad et al. 2012c).

The comparison with other studies depends on the intensity–acceleration conversion. The Nepalese stone-masonry medians of Gautam (2018) lie between the two conversions of the present stone curves (Fig. 10). Under

the relation of Wald et al. (1999) they correspond to intensities 0.6–1.5 degrees below the present stone medians, and under the L&G correlation to intensities 1.1–1.6 degrees above. Within this uncertainty the two stocks are of comparable vulnerability. Intensity-based and acceleration-based fragility functions cannot be compared reliably without a regionally validated conversion. Global models such as that of Martins and Silva (2021) are defined in spectral acceleration and would face the same issue.

3.13 Identifiability from aggregated damage reports

The analysis gives a ladder. The damage of a district constrains intensity plus vulnerability. Given an intensity field, the data determine the vulnerability of the dominant class, here rubble stone, robustly to its prior center and to a terrain term in the intensity bias. The contrast between rubble stone and brick, the two classes whose shares vary most between districts, is not established. Since districts mix classes and terrain, the contrast is an ecological inference (Goodman 1953; King 1997), and intensity errors that follow terrain or composition can produce it. The vulnerabilities of minority classes, here mud and timber, are not identified, and fragility functions or loss estimates that depend on them carry their priors. The absolute level is conditional on the intensity field, here fixed to within about ±0.5 units by the ShakeMap prior and one accelerograph; a damage-free field gives the same stone index within 0.04. Neither more units nor more precise district intensities narrow the class-index intervals much, whereas a known intensity level narrows the stone interval by about a quarter. More units halve the width of the contrast interval; however, they do not protect it from intensity errors aligned with composition. Ioannou et al. (2015) concluded that empirical fragility remains highly uncertain without dense ground-motion recordings in the epicentral area, and the present results quantify that conclusion for aggregated reports. A calibration of this kind should therefore report the five checks of Table 16, which separate the quantities informed by the data from those carried by priors and assumptions.

Table 16 Checks for fragility calibration from aggregated damage reports

Check	Question answered	This study
Posterior-to-prior SD ratio of every parameter and contrast	Which quantities do the data inform?	Table 4
Refit with neutral priors	Do the class contrasts come from the data or from the prior?	Table 5
Refit with an intensity field built without damage observations	Does the result depend on damage-derived intensity?	Table 5
Synthetic data with intensity errors aligned with composition, and a terrain term in the bias	Can aggregation alone produce the contrast?	Sect. 3.6, Table 5
Out-of-sample scores against the prior predictive and deterministic mappings	Does calibration add skill beyond the observation model?	Tables 6 and 11

3.14 Reported categories

The inferred λ and κ show that the reconstruction categories "destroyed" and "damaged" are not interchangeable with EMS-98 grades. Treating "destroyed" as grade 4 or above would bias the fragility functions toward higher vulnerability, whereas ignoring under-reported slight damage would bias them in the opposite direction. The standard mapping, which counts grades 4 and 5 as destroyed and ignores slight damage, makes both assumptions. The dependence of the category on the purpose of the survey is illustrated by the later Detailed Damage Assessment and Beneficiary Eligibility Verification Survey of the Earthquake Reconstruction and Rehabilitation Authority (ERRA). It identified about 463,000 completely destroyed houses eligible for reconstruction grants among about 600,000 destroyed or damaged houses (Arshad and Athar 2013). This is more than twice the 203,579

destroyed dwellings of the preliminary assessment. Part of the difference may reflect counting units and coverage. The grant structure, however, favored classification as destroyed: PKR 175,000 for reconstruction against PKR 80,000 for restoration. Calibration against the eligibility-survey counts would therefore return higher vulnerability indices. The union-council records of that survey are not publicly available. The synthetic tests of Sect. 3.6 suggest that their release would sharpen the reporting parameters and the class contrasts, although not the absolute vulnerability level. On the Indian side, the provisional relief-phase figures differ from the final district counts by factors of up to nine. The final counts can be predicted for fully damaged houses, whereas the partially damaged category differs between the two surveys. Fully damaged counts transfer between surveys better than partial damage does.

3.15 Limitations

On the data side, only eight calibration districts are available, and their counts are preliminary assessments from the relief phase rather than the later ERRA survey, whose union-council records are not public. Since the three AJK districts share one assumed composition, the gap between Bagh (57% destroyed) and Poonch (AJK; 21%) can only be explained by intensity. The "other" wall category is treated as stone, although reassigning up to half of it to brick and block changes the stone index by less than 0.07, and each wall class is treated as homogeneous. The brick and block class includes dwellings with reinforced-concrete frames or roofs, which neither survey separates. Wall material is correlated with terrain and ground failure, which the data cannot separate from vulnerability (Sect. 3.4). The population grid stands in for the distribution of dwellings. The ShakeMap prior is partly derived from damage, and the only independent anchor is a single accelerograph inside a building, although a damage-free intensity field gives the same stone index within 0.04. The Indian damage figures are available for three districts only, the reporting categories of the Indian survey differ from the Pakistani ones, and households rather than dwellings are used as exposure there. Census "wood" walls are not necessarily dhajji-dewari, and the census does not record reinforced-concrete floors.

On the modeling side, MMI, MSK and EMS-98 are treated as equivalent. Q is fixed at 2.3 (2.0 and 2.6 give the same indices within 0.01) and the binomial damage distribution is assumed; the dispersion of the fragility functions is therefore not learned from the data. District deviations are independent, although neighboring districts may share intensity errors; blocked cross-validation gives similar scores. The model was developed through successive versions on the same eight districts, and its out-of-sample scores are therefore partly post hoc. The approach has not been tested by aggregating a building-level damage database, such as that of the 2015 Gorkha earthquake, to administrative units and comparing the result with fragility functions fitted to the individual buildings; the synthetic tests of Sect. 3.6 stand in for this check. The estimate for dhajji-dewari relies on laboratory specimens and depends strongly on the intensity–acceleration correlation (Sect. 3.11.1), and taq could not be quantified.

4 Summary and conclusions

This study investigates what district damage statistics can identify about the seismic vulnerability of Himalayan masonry. District counts of destroyed and damaged dwellings from the 2005 M_w 7.6 Kashmir earthquake, covering 787,583 dwellings in eight districts of Azad Jammu and Kashmir and Khyber Pakhtunkhwa, were combined with census wall-material data, population-weighted ShakeMap intensity and an accelerograph anchor. A hierarchical Bayesian form of the macroseismic method was developed, in which the intensity of each district, the reporting

categories and the district overdispersion were treated as unknown. The identifiability of each parameter was examined with neutral priors, a damage-free intensity field and synthetic data sets, including intensity errors aligned with wall composition. The model was scored by leave-one-district-out and blocked cross-validation against six alternative predictors and tested on the final official damage counts of three districts of Indian Jammu and Kashmir. The calibrated functions were converted to peak ground acceleration, compared with the shake-table capacity of dhajji-dewari and applied to the 2001–2011 change of the housing stock. The following conclusions were drawn from this study:

1. Aggregated damage reports identify a ladder of quantities. Given an intensity field, the vulnerability of the dominant class is determined by the data. The contrast between the two classes whose shares vary most is not established, since intensity errors that follow terrain or composition can produce it. The vulnerabilities of minority classes are not identified. The absolute level is conditional on the intensity field.
2. The calibrated index of Himalayan rubble-stone masonry is 0.96 (90% interval 0.81–1.10), at or slightly above the European reference value of 0.873 (probability 0.82 of exceeding it). It stays between 0.88 and 1.05 in 32 identifiability and sensitivity cases, including neutral priors, an intensity field built without damage observations and a terrain term in the intensity bias, and very heavy damage is its median outcome at intensity VIII. It is conditional on the intensity level: fixing the ShakeMap level 0.5 units lower or higher gives 1.05 or 0.92.
3. From a neutral prior, the data give a probability of 0.93–0.96 that rubble stone is more vulnerable than brick and block masonry, and 0.86–0.90 when a terrain term is added to the intensity bias. With independent intensity errors, such probabilities are about 15 times more likely under a contrast of 0.3 than under none (bootstrap 95% lower bound 5). When the intensity errors follow the stone share as in the real data, spurious contrasts of this strength arise in about one data set in four, nearly as often as a true contrast of 0.3 is detected. The contrast is therefore not established, and, if present, it may partly reflect terrain and ground failure rather than wall material alone.
4. Most of the predictive skill comes from modeling the reporting categories and the uncertainty of the intensity. This improves on reference indices applied at face value in seven of eight districts. The class-structured model also outperforms a single-index model in seven of eight districts, whereas the additional gain from calibration is not significant with eight districts. A systematic intensity bias with distance or intensity is not constrained by the data (posterior-to-prior ratio 0.92).
5. Calibrated on Pakistan alone, the model predicts the final official counts of fully damaged houses in Baramulla and Kupwara, Indian Jammu and Kashmir, within its 90% intervals, and reduces the score of the standard mapping by two-thirds for this category. It under-predicts the partially damaged houses of Kupwara, possibly owing to a more inclusive definition of partial damage, and over-predicts the Punch total. This is a partial out-of-sample test, limited to fully damaged houses in two districts. Joint calibration on both sides of the Line of Control is consistent with the Pakistani estimates.
6. Quadrupling the number of calibration units, as the release of sub-district damage records would, narrows the class intervals by only about 20%, even when the sub-units differ strongly in composition, although it halves the interval of the stone–brick contrast; halving the uncertainty of the district intensities narrows the class intervals by about 5%. Fixing the absolute intensity level narrows the stone interval by about a quarter;

independent constraints on that level, such as additional instrumental records, are therefore about as valuable as much finer damage records.

7. The shake-table capacity of single-story dhajji-dewari corresponds to a vulnerability index of 0.03–0.46 under the correlation of Lagomarsino and Giovinazzi, and 0.47–0.79 under one consistent with Wald et al. It is less vulnerable than rubble stone in both cases and comparable to brick and block masonry in the second, which is the correlation consistent with the intensity scale of the calibration. A regionally validated intensity–acceleration relation is needed. Taq remains unquantified.
8. Between 2001 and 2011, timber-walled houses in Kupwara were replaced by brick and block masonry. This raises the expected share of very heavily damaged houses at intensity VIII for any timber index below about 0.78, which includes all of the mechanical estimates for dhajji-dewari under the L&G correlation and most of them under the Wald-consistent one. Since the damage statistics cannot establish the timber index, this policy-relevant result rests on the mechanical and observational evidence.

Appendix A: Notation

Table A1 Notation

Symbol	Meaning
I, I_{ij}	Macroseismic intensity (EMS-98, MMI and MSK treated as equivalent); true intensity in cell j of district i
SM_{ij}	ShakeMap Atlas intensity of population cell j in district i
V, V_c, V_c^*	Vulnerability index; index of wall class c; representative typology value (Table 2)
ΔV_R, ε_c	Regional modifier common to all classes; class-specific deviation
Q	Ductility index (2.3)
μ_D, p_k, D_k	Mean damage grade; probability of EMS-98 damage grade D_k, $k = 0, \ldots, 5$
λ, κ	Share of grade-3 dwellings reported destroyed; share of grade-1 dwellings reported damaged
λ_{IN}, κ_{IN}	The same for the Indian relief survey (model C)
α	Concentration of the Dirichlet-multinomial likelihood (overdispersion)
b_0, b_1	ShakeMap level bias; contrast (or distance) bias
η_i, s_i	District intensity deviation; its prior SD (population-weighted ShakeMap SD)
w_{ij}, m_{ic}	Population share of cell j; share of wall class c in district i
$P_{i,r}$	Probability that a dwelling of district i is reported in category r
R	Rupture distance (km)
θ_k, σ_k	Median intensity and dispersion of the fragility function for grade D_k
a_y, T, μ, c_1, c_2, S, T_C	Yield spectral acceleration, period, ductility, intensity–acceleration correlation parameters, soil factor and corner period (Eq. 10)
CRPS	Continuous ranked probability score
Model A, B, C	Headquarters-intensity model; population-weighted model with bias terms and anchor; model B calibrated jointly with Indian districts

References

ADB and World Bank (2005) Pakistan 2005 earthquake: preliminary damage and needs assessment. Asian Development Bank and World Bank, Islamabad, 12 November 2005

AFP (2005) Quake destroyed 40,000 homes in Kashmir: official. The Daily Star, 13 October 2005

Ahmad B, Alam A, Bhat MS, Ahmad S, Shafi M, Rasool R (2017) Seismic risk reduction through indigenous architecture in Kashmir Valley. Int J Disaster Risk Reduct 21:110–117. https://doi.org/10.1016/j.ijdrr.2016.11.005

Ahmad N, Ali Q, Umar M (2012a) Simplified engineering tools for seismic analysis and design of traditional Dhajji-Dewari structures. Bull Earthq Eng 10:1503–1534. https://doi.org/10.1007/s10518-012-9364-9

Ahmad N, Ali Q, Umar M (2012b) Seismic vulnerability assessment of multistory timber braced frame traditional masonry structures. Adv Mater Res 601:168–172. https://doi.org/10.4028/www.scientific.net/AMR.601.168

Ahmad N, Ali Q, Ashraf M, Alam B, Naeem A (2012c) Seismic vulnerability of the Himalayan half-dressed rubble stone masonry structures, experimental and analytical studies. Nat Hazards Earth Syst Sci 12:3441–3454. https://doi.org/10.5194/nhess-12-3441-2012

Ali Q, Schacher T, Ashraf M, Alam B, Naeem A, Ahmad N, Umar M (2012) In-plane behavior of the Dhajji-Dewari structural system (wooden braced frame with masonry infill). Earthq Spectra 28:835–858. https://doi.org/10.1193/1.4000051

Ali Q, Khan AN, Ashraf M, Ahmed A, Alam B, Ahmad N, Javed M, Rahman S, Fahim M, Umar M (2013) Seismic performance of stone masonry buildings used in the Himalayan belt. Earthq Spectra 29:1159–1181. https://doi.org/10.1193/091711eqs228m

Ali Q, Ahmad N, Ashraf M, Rashid M, Schacher T (2017) Shake table tests on single-story Dhajji Dewari traditional buildings. Int J Archit Herit 11:1046–1059. https://doi.org/10.1080/15583058.2017.1338789

Ali Q, Ahmad N, Ashraf M, Schacher T (2021) Seismic performance evaluation of two-story Dhajji-dewari traditional structure. Int J Archit Herit 16:1233–1251. https://doi.org/10.1080/15583058.2021.1875081

Allen TI, Wald DJ, Worden CB (2012) Intensity attenuation for active crustal regions. J Seismol 16:409–433. https://doi.org/10.1007/s10950-012-9278-7

Arshad S, Athar S (2013) Rural housing reconstruction program post-2005 earthquake: learning from the Pakistan experience. A manual for post-disaster housing program managers. World Bank and GFDRR, Washington DC, Report 77907

Bilham R (2009) The seismic future of cities. Bull Earthq Eng 7:839–887. https://doi.org/10.1007/s10518-009-9147-0

Bilham R, Gaur VK, Molnar P (2001) Himalayan seismic hazard. Science 293:1442–1444. https://doi.org/10.1126/science.1062584

Bothara J, Hiçyılmaz K (2008) General observations of building behaviour during the 8th October 2005 Pakistan earthquake. Bull N Z Soc Earthq Eng 41:209–233. https://doi.org/10.5459/bnzsee.41.4.209-233

Del Gaudio C, De Martino G, Di Ludovico M, Manfredi G, Prota A, Ricci P, Verderame GM (2017) Empirical fragility curves from damage data on RC buildings after the 2009 L'Aquila earthquake. Bull Earthq Eng 15:1425–1450. https://doi.org/10.1007/s10518-016-0026-1

Dhandapany D, Menon A (2019) Seismic behavior of timber-laced masonry structures in the Himalayan belt. In: Structural Analysis of Historical Constructions, RILEM Bookseries, Springer, pp 605–613. https://doi.org/10.1007/978-3-319-99441-3_65

Durrani AJ, Elnashai AS, Hashash YMA, Kim SJ, Masud A (2005) The Kashmir earthquake of October 8, 2005: a quick look report. Mid-America Earthquake Center Report 05-04, University of Illinois at Urbana-Champaign

EERI (2005) First report on the Kashmir earthquake of October 8, 2005. EERI Special Earthquake Report, Learning from Earthquakes, December 2005. Earthquake Engineering Research Institute, Oakland

EERI (2006) The Kashmir earthquake of October 8, 2005: impacts in Pakistan. EERI Special Earthquake Report, Learning from Earthquakes, February 2006. Earthquake Engineering Research Institute, Oakland

Fayaz M, Romshoo SA, Rashid I, Chandra R (2023) Earthquake vulnerability assessment of the built environment in the city of Srinagar, Kashmir Himalaya, using a geographic information system. Nat Hazards Earth Syst Sci 23:1593–1611. https://doi.org/10.5194/nhess-23-1593-2023

FBS (n.d.) Pakistan Social and Living Standards Measurement Survey 2004–05, district-level report, Table 4.3: percent distribution of households by material used for walls. Federal Bureau of Statistics (now Pakistan Bureau of Statistics), Islamabad

Gautam D (2018) Observational fragility functions for residential stone masonry buildings in Nepal. Bull Earthq Eng 16:4661–4673. https://doi.org/10.1007/s10518-018-0372-2

Gelman A, Rubin DB (1992) Inference from iterative simulation using multiple sequences. Stat Sci 7:457–472. https://doi.org/10.1214/ss/1177011136

Giordano N, De Luca F, Sextos A, Ramirez Cortes F, Fonseca Ferreira C, Wu J (2021) Empirical seismic fragility models for Nepalese school buildings. Nat Hazards 105:339–362. https://doi.org/10.1007/s11069-020-04312-1

Gneiting T, Raftery AE (2007) Strictly proper scoring rules, prediction, and estimation. J Am Stat Assoc 102:359–378. https://doi.org/10.1198/016214506000001437

Goodman LA (1953) Ecological regressions and behavior of individuals. Am Sociol Rev 18:663–664. https://doi.org/10.2307/2088121

Government of India (2005) Situation report on earthquake in Jammu and Kashmir and other parts of Northern India and related relief measures, 22:00 hrs 21 October 2005. Ministry of Home Affairs, New Delhi (via ReliefWeb)

Grünthal G (ed) (1998) European Macroseismic Scale 1998 (EMS-98). Cahiers du Centre Européen de Géodynamique et de Séismologie 15, Luxembourg

Haario H, Saksman E, Tamminen J (2001) An adaptive Metropolis algorithm. Bernoulli 7:223–242. https://doi.org/10.2307/3318737

Harathi KT, Choudhury T (2026) Seismic performance assessment of timber-laced masonry: a numerical study of Dhajji-Dewari and Kath-Kuni walls. In: Structural Analysis of Historical Constructions. RILEM Bookseries. Springer, Cham, pp 1651–1664. https://doi.org/10.1007/978-3-032-16767-5_129

Hough SE, Bilham R, Bhat I (2009) Kashmir Valley megaearthquakes. Am Sci 97:42–49. https://doi.org/10.1511/2009.76.42

Ioannou I, Douglas J, Rossetto T (2015) Assessing the impact of ground-motion variability and uncertainty on empirical fragility curves. Soil Dyn Earthq Eng 69:83–92. https://doi.org/10.1016/j.soildyn.2014.10.024

Ioannou I, Chandler RE, Rossetto T (2020) Empirical fragility curves: the effect of uncertainty in ground motion intensity. Soil Dyn Earthq Eng 129:105908. https://doi.org/10.1016/j.soildyn.2019.105908

Jaiswal K, Wald D, D'Ayala D (2011) Developing empirical collapse fragility functions for global building types. Earthq Spectra 27:775–795. https://doi.org/10.1193/1.3606398

Jaiswal K, Wald DJ (2010) An empirical model for global earthquake fatality estimation. Earthq Spectra 26:1017–1037. https://doi.org/10.1193/1.3480331

Kaneda H, Nakata T, Tsutsumi H, Kondo H, Sugito N, Awata Y, Akhtar SS, Majid A, Khattak W, Awan AA, Yeats RS, Hussain A, Ashraf M, Wesnousky SG, Kausar AB (2008) Surface rupture of the 2005 Kashmir, Pakistan, earthquake and its active tectonic implications. Bull Seismol Soc Am 98:521–557. https://doi.org/10.1785/0120070073

Kim SJ, Elnashai AS (2009) Characterization of shaking intensity distribution and seismic assessment of RC buildings for the Kashmir (Pakistan) earthquake of October 2005. Eng Struct 31:2998–3015. https://doi.org/10.1016/j.engstruct.2009.08.001

King G (1997) A solution to the ecological inference problem: reconstructing individual behavior from aggregate data. Princeton University Press, Princeton

Knodel E, Wald DJ, Quitoriano V, Loos S (2026) The intensity gap: a global analysis of who responds to the crowdsourced "Did You Feel It?" system. Seismol Res Lett 97:2082–2106. https://doi.org/10.1785/0220250168

Koutsourelakis PS (2010) Assessing structural vulnerability against earthquakes using multi-dimensional fragility surfaces: a Bayesian framework. Probabilistic Eng Mech 25:49–60. https://doi.org/10.1016/j.probengmech.2009.05.005

Lagomarsino S, Giovinazzi S (2006) Macroseismic and mechanical models for the vulnerability and damage assessment of current buildings. Bull Earthq Eng 4:415–443. https://doi.org/10.1007/s10518-006-9024-z

Lagomarsino S, Cattari S, Ottonelli D (2021) The heuristic vulnerability model: fragility curves for masonry buildings. Bull Earthq Eng 19:3129–3163. https://doi.org/10.1007/s10518-021-01063-7

Lallemant D, Kiremidjian A, Burton H (2015) Statistical procedures for developing earthquake damage fragility curves. Earthq Eng Struct Dyn 44:1373–1389. https://doi.org/10.1002/eqe.2522

Langenbach R (1990) Of taq and dhajji dwari: the earthquake resistant mud and brick architecture of Kashmir. In: Agnew N, Taylor M, Alva Balderrama A, Houben H (eds) 6th International Conference on the Conservation of Earthen Architecture: Adobe 90 Preprints, Las Cruces, New Mexico. Getty Conservation Institute, Los Angeles

Loos S, Lallemant D, Baker J, McCaughey J, Yun SH, Budhathoki N, Khan F, Singh R (2020) G-DIF: a geospatial data integration framework to rapidly estimate post-earthquake damage. Earthq Spectra 36:1695–1718. https://doi.org/10.1177/8755293020926190

Maqsood ST, Schwarz J (2008) Analysis of building damage during the 8 October 2005 earthquake in Pakistan. Seismol Res Lett 79:163–177. https://doi.org/10.1785/gssrl.79.2.163

Martins L, Silva V (2021) Development of a fragility and vulnerability model for global seismic risk analyses. Bull Earthq Eng 19:6719–6745. https://doi.org/10.1007/s10518-020-00885-1

Musson RMW, Grünthal G, Stucchi M (2010) The comparison of macroseismic intensity scales. J Seismol 14:413–428. https://doi.org/10.1007/s10950-009-9172-0

Naseer A, Khan AN, Hussain Z, Ali Q (2010) Observed seismic behavior of buildings in northern Pakistan during the 2005 Kashmir earthquake. Earthq Spectra 26:425–449. https://doi.org/10.1193/1.3383119

ORGI (2001a) Census of India 2001, Table H-3B Appendix: distribution of households living in census houses by predominant material of wall, Jammu and Kashmir. Office of the Registrar General and Census Commissioner, India

ORGI (2001b) Census of India 2001, Table H-3B: distribution of census houses by predominant material of wall, Jammu and Kashmir. Office of the Registrar General and Census Commissioner, India

ORGI (2001c) Census of India 2001, Primary Census Abstract, Jammu and Kashmir. Office of the Registrar General and Census Commissioner, India

ORGI (2011) Census of India 2011, Table HH-02B: households by predominant material of wall of census houses occupied by them, Jammu and Kashmir. Office of the Registrar General and Census Commissioner, India

Ornthammarath T, Warnitchai P, Maruyama Y, Pornsopin P, Yamazaki F (2025) Far-field ground motion characteristics of the Bangkok Basin, Thailand, in the 2025 M_w 7.7 Mandalay earthquake: initial insights. Bull Earthq Eng 23:6577–6602. https://doi.org/10.1007/s10518-025-02295-7

Qader W, Bhat IM, Qurashi M (2026) Looming seismic threat: a comprehensive review of earthquake hazard in the Kashmir Valley, North-western Himalaya, India. Proc Indian Natl Sci Acad. https://doi.org/10.1007/s43538-026-00692-3

Rafi MM, Ahmed M, Lodi SH, Varum H, Arshad MT, Alam N (2023) Development of fragility functions for brick masonry structures using damage data from September 24, 2019, earthquake in Mirpur, Azad Kashmir. J Perform Constr Facil 37(4):04023029. https://doi.org/10.1061/JPCFEV.CFENG-4441

Rai DC, Murty CVR (2006) Effects of the 2005 Muzaffarabad (Kashmir) earthquake on built environment. Curr Sci 90:1066–1070

Rossetto T, Elnashai A (2003) Derivation of vulnerability functions for European-type RC structures based on observational data. Eng Struct 25:1241–1263. https://doi.org/10.1016/S0141-0296(03)00060-9

Rossetto T, Peiris N (2009) Observations of damage due to the Kashmir earthquake of October 8, 2005 and study of current seismic provisions for buildings in Pakistan. Bull Earthq Eng 7:681–699. https://doi.org/10.1007/s10518-009-9118-5

Rossetto T, Ioannou I, Grant DN, Maqsood T (2014) Guidelines for empirical vulnerability assessment. GEM Technical Report 2014-11, GEM Foundation, Pavia

Rosti A, Rota M, Penna A (2021) Empirical fragility curves for Italian URM buildings. Bull Earthq Eng 19:3057–3076. https://doi.org/10.1007/s10518-020-00845-9

Rota M, Penna A, Strobbia CL (2008) Processing Italian damage data to derive typological fragility curves. Soil Dyn Earthq Eng 28:933–947. https://doi.org/10.1016/j.soildyn.2007.10.010

Silva V, Crowley H, Pagani M, Monelli D, Pinho R (2014) Development of the OpenQuake engine, the Global Earthquake Model's open-source software for seismic risk assessment. Nat Hazards 72:1409–1427. https://doi.org/10.1007/s11069-013-0618-x

Straub D, Der Kiureghian A (2008) Improved seismic fragility modeling from empirical data. Struct Saf 30:320–336. https://doi.org/10.1016/j.strusafe.2007.05.004

Szeliga W, Hough S, Martin S, Bilham R (2010) Intensity, magnitude, location, and attenuation in India for felt earthquakes since 1762. Bull Seismol Soc Am 100:570–584. https://doi.org/10.1785/0120080329

Tatem AJ (2017) WorldPop, open data for spatial demography. Sci Data 4:170004. https://doi.org/10.1038/sdata.2017.4

Thakur VC, Jayangondaperumal R, Champatiray PK, Bhat MI, Malik MA (2006) 8 October, 2005 Muzaffarabad earthquake and seismic hazard assessment of Kashmir gap in northwestern Himalaya. J Geol Soc India 68:187–200. https://doi.org/10.17491/jgsi/2006/680204

UNI (2006) Over 400 crore disbursed as earthquake relief in J and K (reply of the Minister for Revenue and Rehabilitation in the J&K Legislative Assembly). OneIndia, 15 March 2006. https://www.oneindia.com/2006/03/15/over-400-crore-disbursed-as-eathquake-relief-in-j-and-k-1142420863.html

USGS (2020) ShakeMap Atlas, event usp000e12e, M7.6 Pakistan, 8 October 2005 (ShakeMap 4.0.2). U.S. Geological Survey, Earthquake Hazards Program. https://earthquake.usgs.gov/earthquakes/eventpage/usp000e12e/shakemap

Vehtari A, Gelman A, Gabry J (2017) Practical Bayesian model evaluation using leave-one-out cross-validation and WAIC. Stat Comput 27:1413–1432. https://doi.org/10.1007/s11222-016-9696-4

Wald DJ, Quitoriano V, Heaton TH, Kanamori H (1999) Relationships between peak ground acceleration, peak ground velocity, and Modified Mercalli Intensity in California. Earthq Spectra 15:557–564. https://doi.org/10.1193/1.1586058

Worden CB, Gerstenberger MC, Rhoades DA, Wald DJ (2012) Probabilistic relationships between ground-motion parameters and Modified Mercalli Intensity in California. Bull Seismol Soc Am 102:204–221. https://doi.org/10.1785/0120110156

Worden CB, Thompson EM, Hearne M, Wald DJ (2020) ShakeMap manual online: technical manual, user's guide, and software guide. U.S. Geological Survey. https://doi.org/10.5066/F7D21VPQ

Statements and Declarations

Funding This research received no specific grant from any funding agency in the public, commercial or not-for-profit sectors.

Competing interests The author declares that there are no competing interests.

Ethics approval Not applicable. The study uses published, aggregated data only.

Data availability The source data are public: ADB and World Bank (2005); USGS ShakeMap Atlas, event usp000e12e; FBS PSLM 2004–05; Census of India 2001 and 2011; J&K Legislative Assembly reply of 15 March

2006; WorldPop 2005; GADM 4.1. The extracted district data, the derived results and the posterior samples are deposited in Zenodo (https://doi.org/10.5281/zenodo.23661190).

Code availability The analysis code (Python) is deposited with the data in Zenodo (https://doi.org/10.5281/zenodo.23661190).

Author contributions Syed Sajid Hussain is the sole author: conceptualisation, data curation, methodology, software, formal analysis, visualisation, writing – original draft, and writing – review and editing.